Environmental Pollution 265 (2020) 114928

Contents lists available at ScienceDirect

Environmental Pollution

journal homepage: www.elsevier.com/locate/envpol

Comparative toxicometabolomics of perfluorooctanoic acid (PFOA) and next-generation perfluoroalkyl substances☆

Kiflom Y. Gebreab [a], Muhamed N.H. Eeza [b, c], Tianyu Bai [b, c], Zain Zuberi [d], Jörg Matysik [c], Kevin E. O'Shea [a], A. Alia [b, e], John P. Berry [a, *]

[a] Department of Chemistry and Biochemistry, Florida International University, Miami, FL, USA
[b] Institute for Medical Physics and Biophysics, University of Leipzig, Leipzig, Germany
[c] Institute for Analytical Chemistry, University of Leipzig, Leipzig, Germany
[d] The School of Pharmacy and Pharmaceutical Sciences, Trinity College, Dublin, Ireland
[e] Leiden Institute of Chemistry, Leiden University, 2333, Leiden, the Netherlands

ARTICLE INFO

Article history:
Received 27 January 2020
Received in revised form
8 May 2020
Accepted 31 May 2020
Available online 4 June 2020

Keywords:
Perfluoroalkyl substances
Perfluorooctanoic acid
Zebrafish embryo
Toxicity
High-resolution magic angle spin (HRMAS)
NMR metabolomics

ABSTRACT

Owing to environmental health concerns, a number of per- and polyfluoroalkyl substances (PFAS) have been phased-out, and increasingly replaced by various chemical analogs. Most prominent among these replacements are numerous *perfluoroether carboxylic acids* (PFECA). Toxicity, and environmental health concerns associated with these next-generation PFAS, however, remains largely unstudied. The zebrafish embryo was employed, in the present study, as a toxicological model system to investigate toxicity of a representative sample of PFECA, alongside perfluorooctanoic acid (PFOA) as one of the most widely used, and best studied, of the "legacy" PFAS. In addition, *high-resolution magic angle spin* (HRMAS) NMR was utilized for metabolic profiling of intact zebrafish embryos in order to characterize metabolic pathways associated with toxicity of PFAS. Acute embryotoxicity (i.e., lethality), along with impaired development, and variable effects on locomotory behavior, were observed for all PFAS in the zebrafish model. Median lethal concentration (LC_{50}) was significantly correlated with alkyl chain-length, and toxic concentrations were quantitatively similar to those reported previously for PFAS. Metabolic profiling of zebrafish embryos exposed to selected PFAS, specifically including PFOA and two representative PFECA (i.e., GenX and PFO3TDA), enabled elaboration of an integrated model of the metabolic pathways associated with toxicity of these representative PFAS. Alterations of metabolic profiles suggested targeting of hepatocytes (i.e., hepatotoxicity), as well as apparent modulation of neural metabolites, and moreover, were consistent with a previously proposed role of mitochondrial disruption and peroxisome proliferator-activated receptor (PPAR) activation as reflected by dysfunctions of carbohydrate, lipid and amino acid metabolism, and consistent with a previously proposed contribution of PFAS to *metabolic syndrome*. Taken together, it was generally concluded that toxicity of PFECA is quantitatively and qualitatively similar to PFOA, and these analogs, likewise, represent potential concerns as environmental toxicants.

1. Introduction

Per- and polyfluoroalkyl substances (PFAS) are environmental pollutants of emerging concern. Chemically speaking, the PFAS are a class of highly fluorinated organic compounds in which all, or most, hydrogen atoms of "long" (≥6 carbon) or "short" aliphatic chains are substituted by fluorine, and to which terminal polar functionalities (e.g., carboxylic acid, sulfonate) are typically added (Fig. S1) in order to impart highly effective surfactant properties (Prevedouros et al., 2006; Wang et al., 2017). Owing to these properties, the PFAS have been extensively used since the late 1940s in a range of industrial and consumer applications including textiles, household products (e.g., Teflon), cosmetics, firefighting foams, medical devices, oil production, pesticide formulations, and in water-repellants (KEMI, 2015; Prevedouros et al., 2006; Wang et al., 2013).

Due to chemical recalcitrance bestowed by C–F bonds, PFAS are

☆ This paper has been recommended for acceptance by Sarah Harmon.

* Corresponding author. 354 Marine Science Building, Florida International University, 3000 NE 151th Street, North Miami, FL, 33181, USA.
E-mail address: berryj@fiu.edu (J.P. Berry).

https://doi.org/10.1016/j.envpol.2020.114928
0269-7491/

also highly persistent, and potentially bioaccumulative (Prevedouros et al., 2006; Wang et al., 2017), and have been widely detected in the environment, wildlife and humans (Giesy and Kannan, 2001; Prevedouros et al., 2006; KEMI, 2015; Wang et al., 2017). Concentrations of PFAS in drinking water, for example, typically range from ≤200 ng/L to a several parts-per-billion (ppb, i.e., μg L^{-1}) (Sunderland et al., 2019). Levels of PFAS in fish and seafood has, in turn, been generally reported in the range of a few to hundreds ppb (i.e., ng g^{-1}), and has suggested, in fact, to be the primary non-occupational route of human exposure to PFAS (Domingo and Nadal, 2017; Fair et al., 2019). Moreover, studies by the Center Disease Control (CDC) reported detection of PFAS in as much as 98% of the U.S. population (Sunderland et al., 2019) with typical serum concentrations of a few ppb, but up to parts-per-million (ppm, i.e., mg L^{-1}) among occupationally exposed individuals (Worley et al., 2017; Anderson et al., 2019). Notably, a recent study (Mamsen et al., 2019) found that PFAS can be transferred maternally via placenta to embryo and fetal tissues, reaching ppb levels.

At the same time, PFAS have been demonstrated to have a range of adverse effects relevant to human health including reproductive toxicity, carcinogenicity, hormonal dysfunction, hepato/nephrotoxicity, developmental toxicity, neurotoxicity, immunotoxicity, and pulmonary effects (Lau et al., 2007; Prevedouros et al., 2006; Shrestha et al., 2017; Steenland et al., 2009). One of the notable links to human health – identified through both molecular and epidemiological studies – has been a possible association with *metabolic syndrome* including obesity and dyslipidemia, impairment of glucose tolerance and regulation, and increased blood pressure all of which are linked, in turn, to increased risks of heart disease, stroke and diabetes, although findings in this regard have been collectively inconclusive (Matilla-Santander et al., 2017; Christensen et al., 2019; Sunderland et al., 2019). Based on available data regarding adverse health effects, the U.S. Environmental Protection Agency (EPA) has previously proposed a lifetime health advisory level of 70 ng/L in drinking water, though this has recently been lowered (Sunderland et al., 2019).

Given their persistent and widespread distribution in the environment, and potential for bioaccumulation and toxicity (and consequent adverse health effects), the production and use of several of the most common PFAS including, in particular, long chain (≥6 C) representatives of perfluorocarboxylic acids, such as perfluorooctanoic acid (PFOA; Fig. S1), and perfluoroalkyl sulfonic acids, such as perfluorooctane sulfonate (PFOS), have been phased-out in the United States and Europe (Pérez et al., 2013; Substances and Registry, 2015; Wang et al., 2017). These so-called "legacy" PFAS, however, been largely replaced by a diversity of "next-generation" compounds. Among these are numerous *perfluoroethercarboxylic acids* (PFECA; Fig. S1) in which one or more carbon (i.e., -CF_2-) is replaced by an oxygen – as an ether group - while still enabling similar chemical properties (Health and Services, 2018; Substances and Registry, 2015; Wang et al., 2015). Like legacy PFAS, however, this means PFECA are also highly stable, and recent studies suggest that they are equally persistent, and may similarly bioaccumulate, in the environment (Sun et al., 2016; Wang et al., 2015, 2013) This class of PFAS are, thus, emerging as a potential concern as environmental toxicants (Prevedouros et al., 2006; Wang et al., 2017). To date, however, there remains very limited information on the PFECA with respect to toxicity, and possible environmental health concerns (Wang et al., 2017, 2013). Among the PFECA, in fact, only two of the most commonly used – under the trade names, GenX (Fig. S1) and ADONA (4,8-dioxa-3H-perfluorononanoate) - have been studied with respect to toxicity, and specifically in mammalian (i.e., mice and rat) systems (DeWitt, 2015; Wang et al., 2015).

Zebrafish (*Danio rerio*) and, in particular, early life stages (i.e., embryos and larvae) of the species, have become well established as a vertebrate toxicological model (Berry et al., 2016, 2007; Jaja-Chimedza et al., 2017; Roy et al., 2017; Weiss-Errico et al., 2017; Zuberi et al., 2019). In addition to numerous practical advantages of this system including ease of husbandry and breeding, high fecundity, a small and nearly transparent embryo, and rapid (i.e., ~3–5 day) embryogenesis, the zebrafish embryo - as a toxicological model - is both potentially translational to human health, and moreover, represents access to a wide range of relevant and quantifiable toxiciological endpoints. As such, this model system has been employed to investigate a myriad of environmental toxicants (Berry et al., 2007; Ulhaq et al., 2013; Weiss-Errico et al., 2017; Zuberi et al., 2019). Indeed, zebrafish embryos and larvae - and even adult stages – have been previously used to investigate toxicity and toxicokinetics of PFAS including, in particular, PFOA, PFOS and related compounds (Ulhaq et al., 2013; Vogs et al., 2019; Weiss-Errico et al., 2017; Wen et al., 2019; Zheng et al., 2012). In the present study, we utilized the zebrafish embryo model to evaluate a representative sample of PFECA with respect to their toxicity including acute toxicity (i.e., lethality) and developmental impairment, as well as behavioral endpoints. Although the zebrafish embryo has been used previously to investigate several legacy PFAS (e.g., PFOA, PFOS), the current study is among the first to investigate the toxicity of the PFECA, in general, and in this model system specifically.

Given the considerable promise of the zebrafish embryo model, it is perhaps not surprising that a number of biotechnological advances have evolved alongside the toxicological model. Among these is a wide range of "omics" approaches. Very recently, this has included adaptations of nuclear magnetic resonance (NMR)-based metabolomics techniques for metabolite profiling and imaging in the zebrafish model (Chatzopoulou et al., 2015; Kabli et al., 2009; van Amerongen et al., 2014). In particular, approaches based on *high-resolution magic angle spin* (HRMAS) NMR have shown remarkable potential for metabolomics of *intact* zebrafish (Berry et al., 2016; Chatzopoulou et al., 2015; Kabli et al., 2009; Roy et al., 2017; van Amerongen et al., 2014; Zuberi et al., 2019). Briefly stated, HRMAS NMR utilizes spinning of a sample at the so-called "magic angle" (of 54.74° relative to the magnetic field) to minimize major interactions (specifically dipolar and quadrupolar interactions, and chemical shift anisotropy) that, otherwise, cause broadening of signal (i.e., "chemical shift") peaks, and thus, enables resolution of the chemical shifts of multiple compounds (e.g., metabolites) even within complex biological samples including intact zebrafish embryos. This technique has been previously applied to understanding of metabolic contributions to disease state (Chatzopoulou et al., 2015; van Amerongen et al., 2014), and more recently, metabolic alterations associated with environmental toxicants (Berry et al., 2016; Roy et al., 2017; Zuberi et al., 2019). In the latter case, this approach was specifically applied to several naturally occurring biotoxins (e.g., cyanobacterial toxins, mycotoxins), and enabled facile characterization of integrated pathways of toxicity, and identification of potential metabolic biomarkers of toxin-specific effects (Berry et al., 2016; Roy et al., 2017; Zuberi et al., 2019) In the present study, this state-of-the-art technique was applied to a comparative toxicological investigation of PFECA and PFOA as a means of characterizing pathways and targets of PFAS toward an integrated systems-level model of toxicity in relation to possible health concerns.

2. Materials and methods

2.1. Chemicals

Perfluoroethercarboxylic acids (PFECA) including perfluoro (4-methoxy butanoic) acid (PFMOBA), perfluoro-3,6,9-trioxatridecanoic acid (PFO3TDA), perfluoro-3,6,9-trioxadecanoic acid (PFO3DA), perfluoro (2-methyl-3-oxahexanoic) acid (trademarked commercially under the name "GenX"), perfluoro-3,6-dioxaheptanoic acid (PFO2HpA), 4-(heptafluoroisopropoxy)hexafluorobutanoic acid (PFDMMOBA) and Perfluoro-3,6-dioxadecanoic acid (PFO2DA) were purchased from SynQuest Laboratories (Dallas, TX U.S.A.). Perfluorooctanoic acid (PFOA), and all other chemicals (i.e., deuterated phosphate buffer and reference standard for NMR), were purchased from Sigma-Aldrich (St. Louis, MO, U.S.A.). Stock solutions of PFECAs and PFOA were prepared with deionized water in polypropylene tubes (to prevent adsorption to glass; Shafique et al., 2017), and were sonicated until complete dissolution of the compounds was achieved. All chemicals were utilized without further purification.

2.2. Zebrafish embryo toxicity assays

Zebrafish embryo toxicity of PFAS was assessed as previously described (Berry et al., 2007; Jaja-Chimedza et al., 2017; Weiss-Errico et al., 2017). Evaluation of toxicity was primarily conducted in laboratories at Florida International University under protocols approved by the FIU Animal Care and Use Committee (IACUC). Additional details of rearing and breeding of zebrafish, and toxicity assays, are given in the Supplementary Materials. For comparison to a representative legacy PFAS, the toxicity of PFECA (and subsequent metabolic profiling experiments) was assessed alongside PFOA for which toxicity in the zebrafish embryo model has been previously evaluated (Hagenaars et al., 2011; Weiss-Errico et al., 2017). Preliminary studies enabled establishment of effective concentration ranges for PFAS, and accordingly, embryos (PSA line at $\leq$ 4 h post-fertilization [hpf]) were exposed to a concentration series of 25, 50, 75, 100, 150, 200 ppm for PFMOBA, Gen X, PFO2HPA, PFO3DA and PFOA; 100, 150, 200, 250 and 300 ppm for PFDMMOBA; 5, 10, 50, 75 and 100 ppm for PFO2DA; and 1, 5, 10, 20, 30 and 40 ppm for PFO3TDA.

Embryo toxicity was observed, and recorded, at four developmentally relevant timepoints, i. e., 1, 2, 5 and 7 days post-fertilization (dpf), over 7-d continual exposure. Relevant toxicological endpoints included lethality/mortality, developmental inhibition and neurobehavioral endpoints. With respect to mortality, median lethal concentration (LC_{50}) was calculated for each test compound at each timepoint, based on percent mortality (N = 3 replicates of 5 embryos per well) fitted to sigmoidal concentration-response curves, specifically using Origin 2018b software (Origin Lab, Northampton, Massachusetts, USA) with LC_{50} values calculated by Probit Analysis in SPSS (version 23.0; IBM Corporation Armonk, NY, USA, 2015). Alongside mortality, morphological developmental deformities were recorded by light photomicrography using Olympus DP2-BSW imaging software (Olympus, Center Valley, PA, USA, 2009). Inhibition of development and behavioral dysfunction were assessed, respectively, based on interocular distance (IOD) and vestibular righting reflex (i.e., percent listing in 30 s interval, n = 6) for pooled surviving embryos (at 7 dpf), compared to untreated (E3 medium only) controls, as previously described (Weiss-Errico et al., 2017). One-way ANOVA was used to calculate the statistical significance of differences between LC_{50} values, calculated at each timepoint, and IOD and percent listing (at 7 dpf) relative to untreated (E3 only) controls, for all treatments.

2.3. Exposures for HRMAS-NMR metabolic profiling

Toward comparative characterization of targets and pathways of toxicity, metabolic profiling of zebrafish exposed to three representative PFAS - specifically PFOA, GenX and PFO3TDA – was performed by HRMAS NMR, as previously described (Berry et al., 2016; Roy et al., 2017; Zuberi et al., 2019). All exposures and subsequent NMR analyses were conducted at the University of Leipzig with embryos (OBI/WIK line) provided by the Helmholtz Center for Environmental Research. Prior to NMR metabolomics studies, additional assessments of toxicity were subsequently conducted in laboratories to confirm toxicity in this line, in general, and to determine relevant exposure parameters including sublethal concentrations and optimal developmental stage, for PFAS (i.e., PFOA, GenX and PFO3TDA) selected for metabolomic studies. Details of rearing and breeding of zebrafish, and these additional toxicity assays, are given in the Supplementary Materials. Exposures for NMR analyses were accordingly performed using 72 hpf embryos exposed (in 25 mL of ISO medium (Knöbel et al., 2012) in 75 cm^2 tissue culture flasks) to final concentrations of PFOA, GenX or PFO3TDA, below LC_{50} for these compounds (50, 100 and 10 ppm, respectively), for 24 h, i.e., collected at 96 hpf. Additional exposure replicates were made to account for any losses due to mortality, and in order to generate a sufficient number of embryos (N = 100) and replicates (n = 3) to achieve quantitative NMR analyses. After washing 3 times with MilliQ water to remove residual PFAS, embryos were transferred to 4-mm zirconium oxide rotors (Bruker BioSpin AG, Switzerland) to which 10 μL deuterated phosphate buffer (100 mM, pH 7.0) containing 0.1% (w/v) 3-trimetylsilyl-2,2,3,3-tetradeuteropropionic acid (TSP) was added as a reference (^{1}H chemical shift at 0 ppm).

2.4. HRMAS NMR analysis

All HRMAS NMR experiments were performed on a vertical Bruker magnet (DMX 600-MHz), which was equipped with a 4-mm HRMAS doubly tuned ^{1}H/^{13}C inverse probe with a magic angle gradient. Measurements were carried out at a spinning rate of 6 kHz and a temperature of 277 K which was achieved by a Bruker BVT3000 control unit. Data acquisition and processing were carried out using Bruker TOPSPIN 2.1 software (Bruker Analytische Messtechnik, Germany).

One-dimensional ^{1}H HRMAS NMR spectra were obtained as described previously (Roy et al., 2017). A zgpr pulse sequence (from Bruker's standard pulse program library) with water suppression was used for one-dimensional ^{1}H HR-MAS NMR spectra. Each one-dimensional spectrum was acquired applying a spectral width of 8000 Hz, domain data points of 16k, number of averages of 512 with 8 dummy scans, constant receiver gain of 2048, and acquisition time of 2 s and relaxation delay of 2 s. The relaxation delay was set to a small value to remove short T_2 components due to the presence of lipids in intact embryo samples. All spectra were processed by an exponential window function corresponding to a line broadening of 1 Hz and zero-filled before Fourier Transformation. NMR spectra were phased manually, and automatically baseline corrected using TOPSPIN 2.1 (Bruker Analytische Messtechnik, Germany). The total analysis time (including sample preparation, optimization of NMR parameters and data acquisition) of ^{1}H-HRMAS NMR spectroscopy for each sample was approximately 20 min.

All HRMAS NMR spectra were manually phased, baseline corrected and analyzed using TOPSPIN 4.0.6 (Bruker Analytische Messtechnik, Germany). Quantification of metabolites was performed by Chenomx NMR Suite 8.2 (Chenomx Inc., Edmonton, Alberta, Canada). The concentrations of metabolites were

calculated as a ratio relative to total creatine (tCr), since the external reference may lead to misleading results, and tCr resonance has been previously shown to be a reliable internal reference in a wide range of animal studies. Statistical analysis of metabolite quantification was done by one-way analysis of variance (ANOVA) using OriginPro v. 8 (OriginLab, Northampton, MA, USA), and calculated F-values larger than 2.8 ($p < 0.05$) were considered significant. Multivariate analysis of the one-dimensional NMR spectra were performed as described earlier (Roy et al., 2017; for details, see Supplementary Materials).

3. Results and discussion

3.1. Toxicity of PFECA and PFOA in the zebrafish embryo model

Toxicity of the PFECA and PFOA was evaluated for zebrafish embryos continually exposed over 7 dpf at compound-specific ranges of exposure concentrations. Concentration-dependent toxicity of the PFECA was observed with respect to lethality (Fig. S2) which was accompanied by clear impairment of development and locomotory function. Generally speaking, median lethal concentrations of PFECA (Table 1) were similar to those previously reported for other PFAS, i.e., 10–10^2 μM (Jantzen et al., 2016; Weiss-Errico et al., 2017; Zheng et al., 2012), and LC_{50} values for PFOA were, likewise, comparable to those previously reported (e.g., Ding et al., 2013; Zheng et al., 2012) for this compound (i.e., 261 and 271 ppm, respectively). Although frequency of deformities was not dose-dependent, a range of developmental deformity including bent body axes and edema, as well as general moribundity accompanied by sloughing of dermal layers, was observed in approximately 7–10% of surviving embryos (Fig. S4). No significant effect on hatching rate, however, was observed with >90% hatching observed for both control and treated embryos by 4 dpf (data not shown).

Table 1
Median lethal concentration (LC_{50}) of PFECA and PFOA in the zebrafish embryo model. Calculated values (in μM), along with 95% confidence intervals, are specifically given for 24 h exposure of ≤3 h post-fertilization (hpf) embryos. LC_{50} values were calculated by Probit analysis; dose-response curves are given in Supplementary Materials. Shown, for comparison, are number of fluorocarbons (-CF_x) and ether oxygens (-O-) in the alkyl chain of each PFAS.

	Alkyl Chain		LC_{50} (μM) ± 95% CI
	-CF_x-	-O-	
PFECA			
PFMOBA	5	1	499 ± 0.0
GenX	5	1	383 ± 30
PFDMMOBA	6	1	248 ± 81
PFO2HpA	4	2	441 ± 66
PFO2DA	7	2	157 ± 8
PFO3DA	6	3	202 ± 8
PFO3TDA	9	2	38 ± 6
PFOA	7	0	232 ± 29

Embryo mortality, furthermore, increased for all PFECA and PFOA over the 7 d continuous exposure (Fig. 1): median lethal concentrations significantly decreased between 1 and 7 dpf for 6 of the 7 PFECA including PFMOBA ($p < 0.001$), GenX ($p < 0.0001$), PFO2HpA ($p < 0.001$), PFO2DA ($p < 0.0001$), PFO3DA ($p < 0.001$) and PFO3TDA ($p < 0.0001$), as well as PFOA ($p < 0.001$), and increased most drastically post-hatch (approximately 72 hpf). (Fig. 1). Alongside cumulative toxicity (over total duration of exposure), it is proposed that increased toxicity of PFAS at later embryonic stages may be related to two factors. The first is a development of the liver, and corresponding role hepatic enzyme. Previous studies have demonstrated targeting of hepatocytes by PFAS, and a role of the hepatic *phase I* (i.e., cytochrome P450 [CYP]) and *phase II* enzymes (e.g., glutathione-S-transferase [GST]) has been specifically implicated in a range of mammalian and teleost fish (e.g., carp, rare minnow) models (Cheng and Klaassen, 2008; Liu et al., 2009, 2008; Rotondo et al., 2018). Targeting of hepatocytes by PFECA and PFOA would be consistent with the significant increase in toxicity at later stages of embryo development, as observed in our study (Fig. 1), since it has been shown that differentiation of the liver, and significant expression of relevant enzymes (e.g., CYP), in zebrafish occurs at approximately 72 hpf. A similar increase in acute toxicity has, indeed, been previously demonstrated for recognized hepatotoxins (e.g., aflatoxin, acetaminophen) in the zebrafish embryo model (Pandya et al., 2016; Zuberi et al., 2019). Alternatively, stage-dependent toxicity of the PFECA may be simply related to hatching – which, likewise, occurs at approximately 72 hpf – and specifically, to a role of the chorion as a barrier to these compounds. Recent studies have investigated uptake and toxicokinetics of PFAS in the zebrafish embryo model,

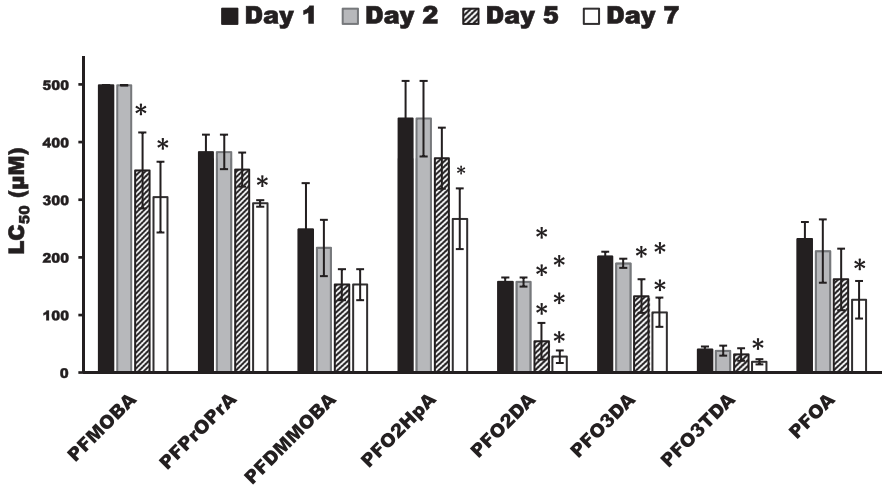

Fig. 1. Increased mortality, as measured by median lethal concentrations (LC_{50}), with continuous exposure of zebrafish embryos to PFECA and PFOA over 7 dpf. Asterisks (i.e., ** and ***) indicate that LC_{50} is significantly different ($p < 0.001$ and $p < 0.0001$) from 1 dpf values. Error bars represent 95% confidence interval.

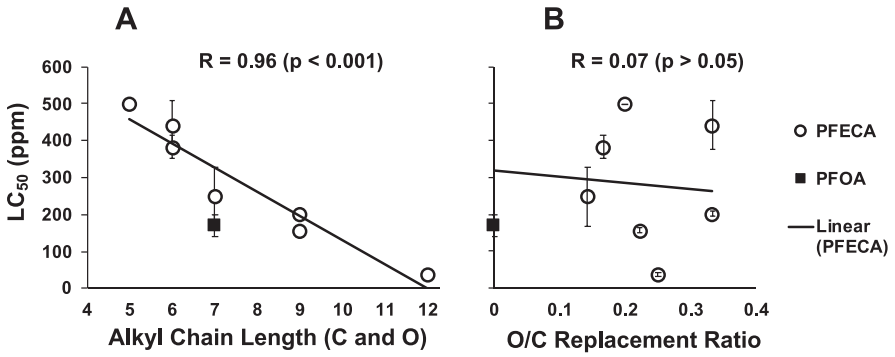

Fig. 2. Correlation between acute embryotoxicity, based on lethality (LC_{50}) at 24 hpf, relative to alkyl chain length (A) and O/C ratio, as a measure of replacement of -CF_2- by ether oxygen, in alkyl chain (B) of PFECA and PFOA. Alkyl chain length is defined as number of carbon and oxygen atoms not including terminal carboxylic acid group. Significant correlation was observed between alkyl chain length and LC_{50}, whereas no significant correlation was observed between LC_{50} and ratio of O/C (i.e., number of ether groups) in the alkyl chain. Pearson correlation coefficient (R), and statistical significance (p-value) are given for correlations.

and concluded a clear contribution of the chorion as a barrier for uptake until approximately 48 hpf after which uptake, as measured by PFAS concentration in post-hatch embryos, steadily increased (Huang et al., 2010; de Koning et al., 2015; Keiter et al., 2016; Vogs et al., 2019).

Embryotoxicity (i.e., LC_{50}) of PFECA was significantly correlated with alkyl-ether chain length of PFECA (Fig. 2). A similar relationship between alkyl chain length and both toxicity, and uptake and bioconcentration, has been consistently reported for other PFAS in numerous previous studies including the zebrafish model (Zheng et al., 2012; Buhrke et al., 2013; Mahapatra et al., 2017; Vogs et al., 2019; Wen et al., 2017). Uptake and subsequent toxicity are presumptively due to the positive correlation between lipophilicity and alkyl-ether chain length which is supported by a generally positive correlation between lipophilicity and uptake previously documented for a diversity of compounds in the zebrafish embryo (Berghmans et al., 2008; de Koning et al., 2015; Jaja-Chimedza et al., 2017). Most notably, the LC_{50} of PFOA generally falls within the same range, relative to chain length, as PFECA (Fig. 2A), whereas the degree of substitution of -CF_2- by ether groups in PFECA (as measured by O/C ratio of PFECA) was not correlated with toxicity (Fig. 2B). Taken together, these findings suggest that while chain length of PFAS (including both PFOA and PFECA) is consistently correlated with embryo toxicity, the replacement of fluorocarbons by ether, as in the PFECA, has no effect on toxicity in the zebrafish embryo (as measured by lethality). This further suggests that acute toxicity (and presumably toxicokinetics, i.e., uptake) are, in fact, quantitatively similar for these next-generation chemical variants.

In addition to lethality, PFECAs and PFOA impaired embryo development as evidenced by morphometric measurements, and specifically IOD (Fig. 3A) as a proxy of embryo size (Weiss-Errico et al., 2017). The effect, however, was independent (in the concentration range tested) of chain-length or any other apparent structural feature. Generally speaking, all PFECA and PFOA significantly ($p < 0.0001$) reduced IOD by nearly 50% (Fig. 3A). A similar decoupling of lethality and morphometrically assessed developmental toxicity was previously observed for PFOA in the zebrafish embryo model (Weiss-Errico et al., 2017).

Finally, alongside lethality and developmental toxicity, several of the PFECA signficantly affected locomotory behavior of exposed zebrafish embryos, specifically measured by righting behavior – and, to be exact, rate of listing - of hatched eleutheroembryos at 7 dpf (Fig. 3B). A similar effect was, in fact, previously reported for PFOA in the zebrafish embryo model (Weiss-Errico et al., 2017). Although 5 of the 7 PFECA, as well as PFOA, significantly increased percent of embryo listing (compared to controls) in the present study, no quantitative relationship between chain length, or any other structural feature of the compounds was discernible. Whether the effect of PFECA and PFOA was due to neurotoxicity – that is modulation of neurochemistry – or simply due to overall developmental toxicity remains to be seen, however, alteration of neural metabolites was, in subsequent metabolic profiling (discussed below), observed in the present study.

3.2. HRMAS NMR metabolic profiling of PFAS-exposed zebrafish embryos

Metabolic profiling of intact zebrafish embryos by HRMAS NMR was undertaken to elucidate targets and pathways associated with toxicity of three representative PFAS which were specifically selected to include a previously well studied representative (i.e., PFOA), and PFECA (i.e., GenX and PFO3TDA) with variable levels of embryo toxicity (i.e., low and high, respectively). More generally, the three compounds represent three levels of toxicity, i.e., PFO3TDA > PFOA > GenX (Table 1 and Fig. S2).

Prior to exposures for metabolomics studies, embryo toxicity was reassessed (see Supplementary Materials and Methods) to confirm relative toxicity, and establish appropriate concentrations and developmental stage for exposures. These assessments established sub-lethal concentrations (Fig. S3) for which embryos were generally indistinguishable from untreated controls, and severely moribund embryos as seen at higher exposure concentrations (Fig. S4), were not observed. Exposure concentrations employed (50, 100 and 10 ppm for PFOA, GenX and PFO3TDA, respectively) were 2–3 orders of magnitude higher than levels typically measured in drinking water, and those measured in human serum, which are typically ppb levels or less (although serum levels as high as 1 ppm have, in fact, been measured in occupationally exposed individuals; Worley et al., 2017; Sunderland et al., 2019). These relatively high (yet sub-lethal) levels were selected, however, to assure a sufficient and significant alteration in metabolomics studies. An exposure window from 72 to 96 hpf was, furthermore, established. At this stage, most relevant organ systems (e.g., liver, kidney) are largely differentiated, and key aspects of CNS development occur, or have occurred, including formation of the midbrain-hindbrain boundary (~27 hpf), and elaboration of telencephalon, mesencephalon, hypothalamus and, importantly, primary and secondary motor neurons (~96 hpf). No apparent developmental effects with respect to these systems were observed during the exposure period (between 72 and 96 hpf) for any of the

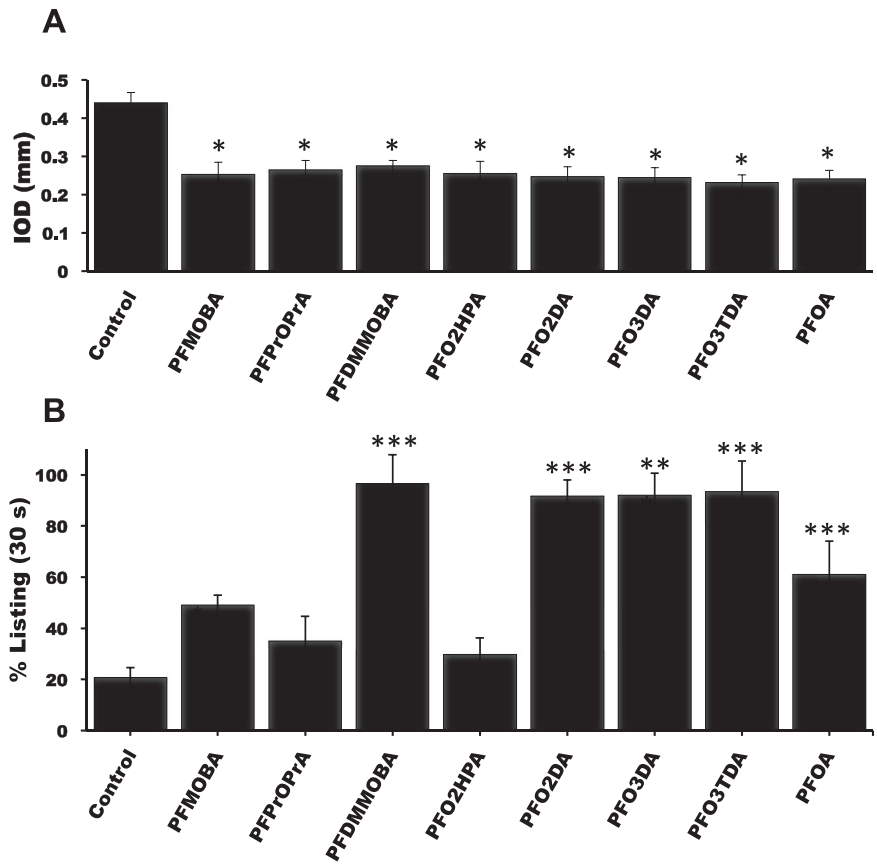

Fig. 3. Developmental impairment and behavioral dysfunction of zebrafish embryos (at 7 dpf) exposed to PFECA and PFOA. (A) Interocular distance (IOD), as a morphometric measure of embryo body size, for surviving embryos exposed to sublethal concentrations (<LC_{50}) of PFECA and PFOA at 7 dpf, compared to controls. The IOD was significantly reduced (***$p < 0.0001$) for embryos exposed to all PFECA and PFOA, compared to controls. (B) Percent listing of surviving embryos exposed to sublethal concentrations (<LC_{50}) of PFECA and PFOA at 7 dpf, compared to controls. Percent listing was significantly higher for embryos exposed to PFDMMOBA, PFO2DA, PFO3DA, PFO3TDA and PFOA (*** = $p < 0.0001$), as well as PFMOBA (**$p < 0.005$). Error bars represent 95% CI.

PFAS tested at these exposure concentrations.

Highly-resolved and reproducible NMR spectra were obtained from intact control and PFAS-treated embryos (Fig. S5), and quantitative analysis revealed significant alteration of 33 metabolites by one or more of the PFAS evaluated (Fig. 4 and Table S1). Principal components analysis, furthermore, showed that metabolic profiles of the three PFAS, and untreated control, could be clearly discerned suggesting a significant quantitative difference in the metabolic profiles affected (Fig. S6). Notably, the percent of metabolites altered was positively correlated with LC_{50} of the PFAS (Fig. 5), suggesting that metabolic effects paralleled acute toxicity. Qualitatively, however, there was considerable overlap in terms of the metabolites affected by exposure. Generally speaking, metabolite levels altered by PFAS could be grouped into several categories including (1) indicators of hepatotoxicity; (2) modulation of neural metabolites and/or pathways; (3) metabolites associated with oxidative stress; and moreover, (4) interrelated carbohydrate, lipid and amino acid metabolism, and associated cellular energetics.

3.3. An integrated system-level model of metabolic targets and pathways of PFAS toxicity

Taken together, the metabolic alterations observed in the present study enabled an integrated model of the metabolic pathways of PFAS toxicity in the zebrafish embryo (Fig. 6). Although the current study is the first to utilize metabolomics of the zebrafish embryo to investigate PFAS - and the first omics study of any PFECA - previous *ex vivo* transcriptomics (Peng et al., 2013), proteomics (Shao et al., 2018) and metabolomics (Peng et al., 2013; Shao et al., 2018; Yu et al., 2016) studies have been conducted for PFOA in other cellular and/or organismal systems. As such, metabolic profiles observed in the present study are perhaps best interpreted relative to this legacy PFAS. That said, metabolites altered by exposure to both PFO3TDA and GenX were quite similar to PFOA (Fig. 4 and Table S1), and the differences between the three representative PFAS could be largely explained based on relative toxicity (Fig. 5). Accordingly, this model could generally, therefore, be extended to the PFECA.

At the organ system (and corresponding cellular) level, several previous studies have suggested that PFAS target liver (i.e., hepatocyte) and kidney due, most likely, to the general role of these organ systems in detoxification and depuration of xenobiotics (Mortensen et al., 2011). Cellular uptake, and consequent tissue distribution, of PFOA has been shown in numerous studies to be specifically facilitated by solute carrier (SLC) transporters that are primarily localized to liver and kidney (Yang et al., 2010; Popovic et al., 2014; Zhao et al., 2016; Kimura et al., 2017). Consistent with targeting of hepatocytes, an observed stage-dependence of PFOA toxicity in the present study coincides (as discussed above) with differentiation (at ~ 72 hpf) of the liver as a target organ. Specifically aligned with hepatotoxicity, PFOA ($p < 0.005$), PFO3TDA ($p < 0.000001$) and GenX ($p < 0.05$) all showed a significant reductions in the molar ratio of branched-chain to aromatic amino acids (BCAA/AAA) relative to negative controls (Table S1). Altered

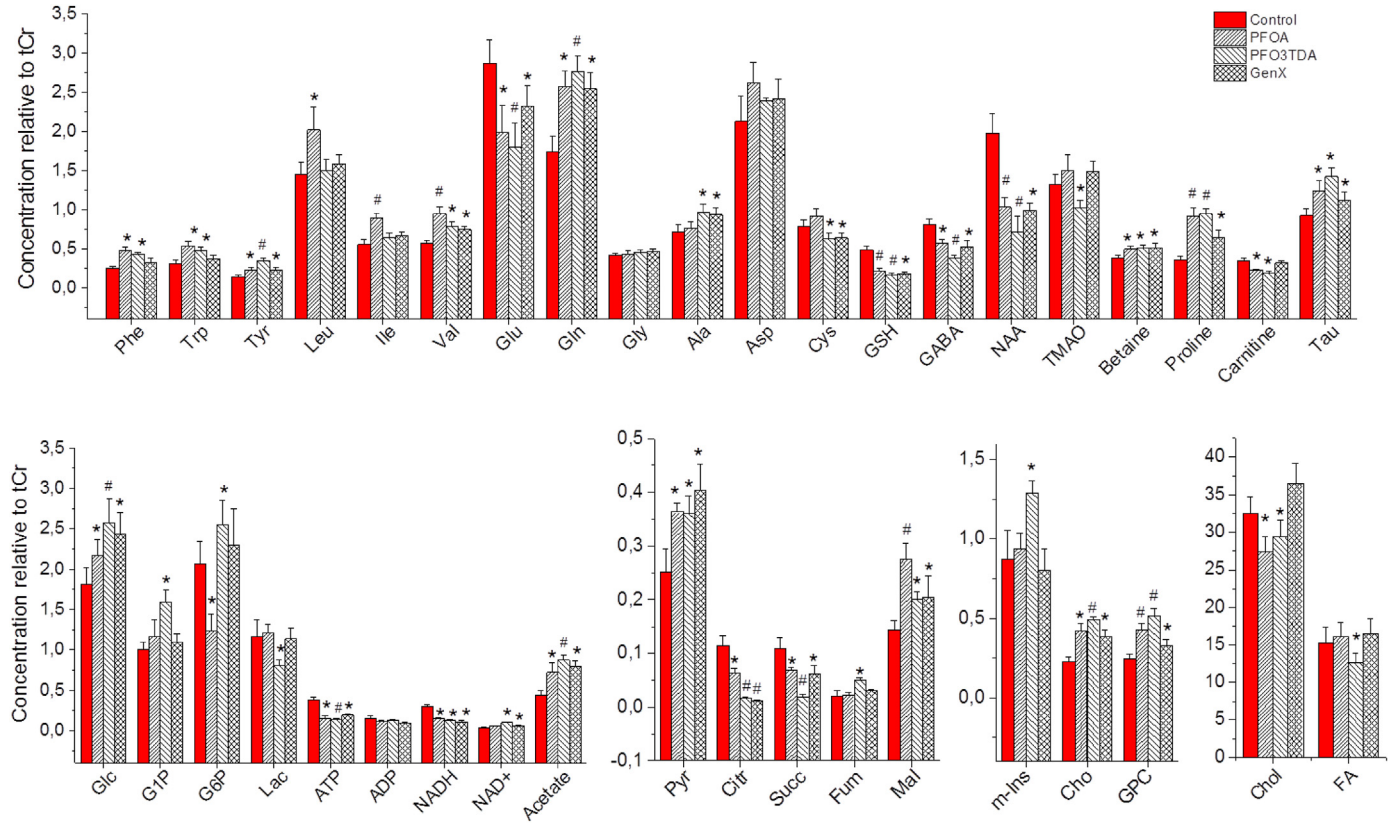

Fig. 4. Effect of PFOA, PFO3TDA and GenX treatment on the metabolic profile of intact zebrafish embryos. Zebrafish embryos (3 dpf) were exposed to 50 ppm PFOA, 10 ppm PFO3TDA or 100 ppm GenX for 24 h. Shown are concentrations of metabolites relative to total creatine (tCr); values are average ± SE of mean. #P < 0.01, *P < 0.05. Abbreviations: Phe = phenylalanine; Trp = tryptophan; Tyr = tyrosine; Leu = leucine, Ile = isoleucine; Val = valine; Glu = glutamate; Gln = glutamine; Gly = glycine; Ala = alanine; Asp = aspartate; Cys = cysteine; GABA = g-aminobutyric acid; GSH = glutathione; Glc = glucose; G1P = glucose-1-phosphate; G6P = glucose-6-phosphate; Lac = lactate; ATP = adenosine triphosphate; ADP = adenosine diphosphate; NADH/NAD+ = reduced/oxidized nicotinamide adenine dinucleotide; m-Ins = *myo*-inositol; Cho = choline; GPC = glycerophosphocholine; Chol = cholesterol; FA = fatty acids.

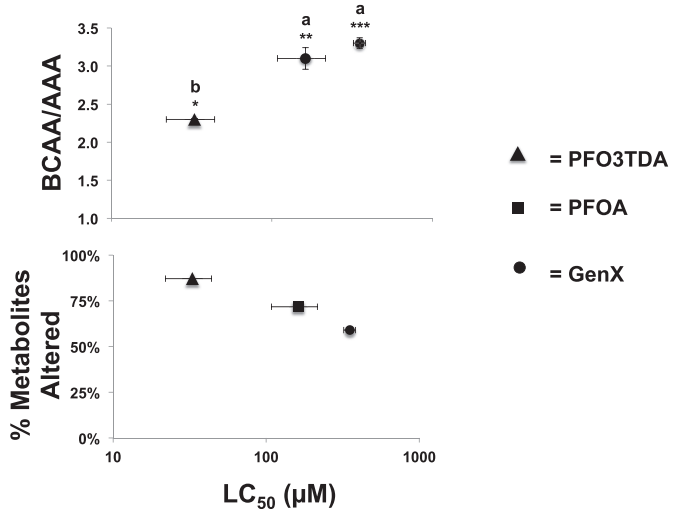

Fig. 5. Change in metabolite levels relative to acute toxicity. Acute toxicity is represented by LC_{50} values for PFAS. Hepatotoxicity (using BCAA/AAA ratio as biomarker) correlated with LC_{50} (A). Similarly, percentage of metabolites altered versus LC_{50} was correlated, suggesting a quantifiable coupling between acute toxicity and level of metabolic effects (B). Asterisks indicate significant difference between treatments and control with respect to BCAA/AAA ratio: *p < 0.05, **p < 0.005, ***p < 0.000005. Letters associated with error bars indicate significant difference (p < 0.05) between treatments with respect to BCAA/AAA ratio (y-error bars) and LC_{50} (x-error bars).

BCAA/AAA ratio is a well-established *ex vivo* (i.e., plasma level) indicator of liver damage (Muratsubaki and Yamaki, 2011), and in similar studies, has been recently found to parallel hepatotoxicity in the intact zebrafish embryo model (Zuberi et al., 2019). Furthermore, BCAA/AAA ratio was significantly correlated with LC_{50}, underscoring hepatocytes as a target of acute toxicity (Fig. 5, Table S1).

Presumably reflective of the relatively higher hepatotoxicity, a significant decrease in trimethylamine *N*-oxide (TMAO) was uniquely observed for PFO3TDA (as the most toxic PFAS tested). TMAO is the product of the oxidation of trimethylamine, exclusively by hepatic *flavin-containing monooxygenase 3* (FMO3), which is, in turn, derived from metabolism of choline and betaine (among other diet-derived precursors) by enteric microbiota (Alfieri et al., 2008; Janeiro et al., 2018; Lang et al., 1998). Choline and betaine, in fact, are typically correlated - as companion biomarkers - with TMAO levels (Janeiro et al., 2018), and were both increased in the present study (for all PFAS treatments). Higher acute hepatotoxicity of PFO3TDA, therefore, is likely to result in a decrease of FMO3 function, and the consequent reduction in TMAO levels observed here. Moreover, TMAO (along with its metabolic precursors, i.e., betaine and choline) has been proposed as a biomarker for *metabolic syndrome* (Barrea et al., 2019; Janeiro et al., 2018), and as such, is perhaps not only reflective of hepatoxicity, but thus, also aligns with the reported link between PFAS and metabolic syndrome (Matilla-Santander et al., 2017; Christensen et al., 2019), and numerous metabolic alterations observed in the present study

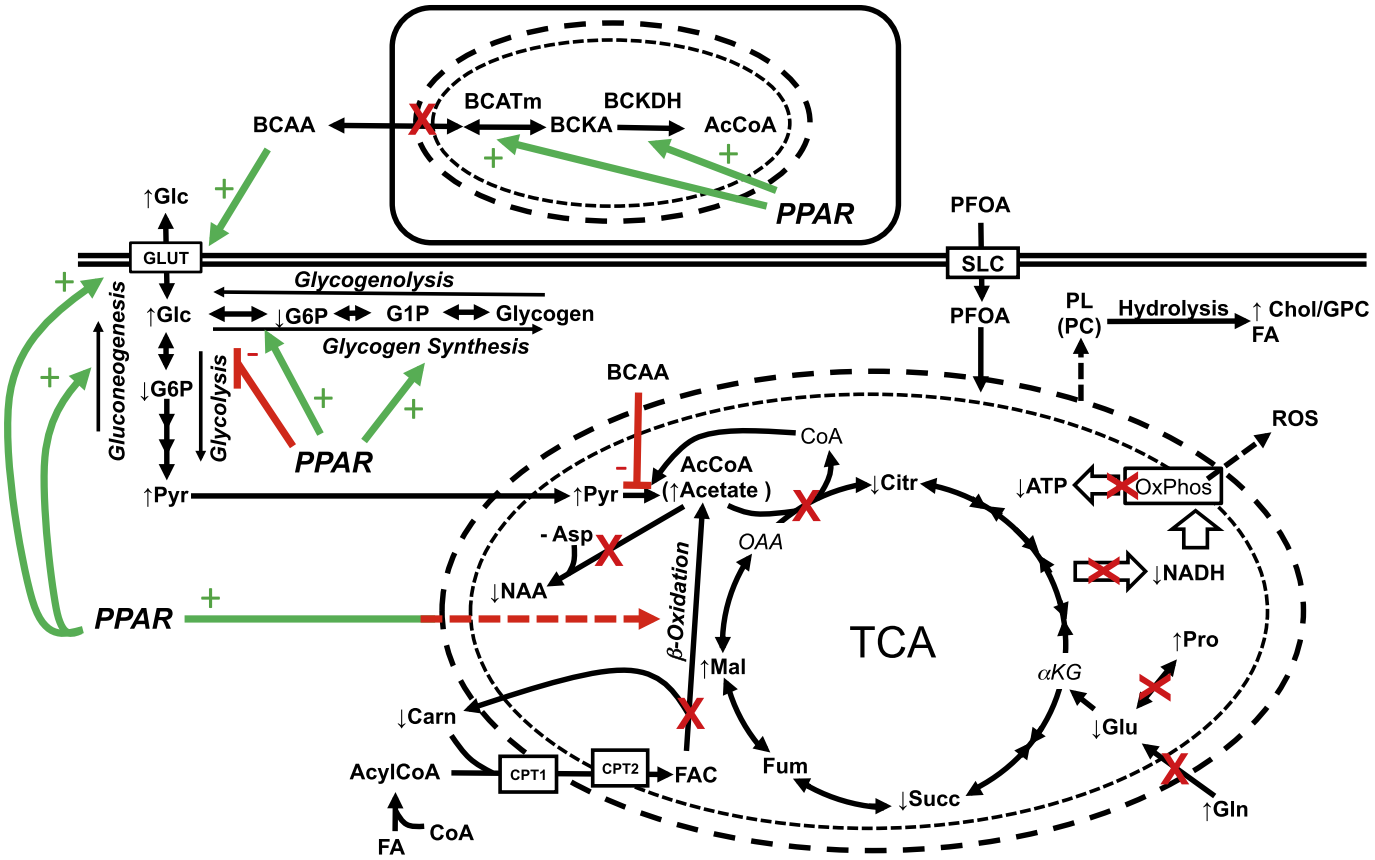

Fig. 6. A model of the targeting of mitochondria and PPAR by PFOA in relation to changes in metabolic alterations. Abbreviations: TCA = Tricarboxylic acid cycle, i.e., citric acid cycle; PPAR = peroxisome proliferator-activated receptor; BCAA = branch-chained amino acids; BCATm = branch-chained amino acid aminotransferase; BCKA = branch-chained keto acid; BCKDH = branch-chained alpha-keto acid dehydrogenase; AcCoA = acetyl CoA; CPT1 and CPT2 = carnitine palmitoyl transferase I and II; FAC = fatty acyl carnitine; OxPhos = oxidative phosphorylation; ROS = reactive oxygen species; PL = phospholipids; PC = phosphatidylcholine; SLC = solute carrier transport protein; α-KG = alpha-ketoglutarate; GLUT = glucose transporter; for other metabolite abbreviations, see Fig. 4.

related to cellular energetics, glucose homeostasis and dyslipidemia (as discussed below).

A significant decrease in GSH (Fig. 4) may, furthermore, correlate with targeting of hepatocytes by PFOA. Although GSH is a ubiquitous antioxidant in biological systems, it is particularly associated with Phase II detoxification which is localized to the liver, and numerous studies have similarly reported decreases in GSH in association with hepatotoxicity (Maddox et al., 2009; Song et al., 2003). That said, a decrease in GSH may be more generally linked to the well-established induction of oxidative stress by PFAS mediated by mitochondrial impairment (Hagenaars et al., 2013; Liu et al., 2007; Tang et al., 2018).

Although liver and kidney have been most frequently linked to PFOA toxicity, there is a considerable body of evidence to suggest that neuronal dysfunction may contribute to deleterious effects (Johansson et al., 2008). Behavioral impairment (Fig. 3B) observed in the current study is consistent with effects on neural systems, and several metabolites affected by PFAS are, likewise, aligned with possible neurotoxicity and/or neurodevelopmental toxicity (Fig. 4). Among these, levels of the metabolically interrelated neurotransmitters, Glu and GABA, were significantly reduced with exposure to PFAS. At the same time, the concentration of NAA which is uniquely associated with (and one of the most abundant metabolites, second only to Glu, in) neural cells was significantly decreased. Biosynthesized from Asp and acetyl CoA in the mitochondria of neural cells, the observed decrease in NAA would be consistent with not only general targeting of neural cells, but specifically mitochondria (discussed below; Fig. 5). Alterations of NAA have, furthermore, been recently proposed as a biomarker of disruption of the interaction between neurons and glial cells including myelination, i.e., oligodendrocyte/neuron interactions (Xu et al., 2016). Interestingly, the ratio of Gln/Glu (which was increased in PFAS-treated embryos) has been, likewise, suggested to be a metabolic indicator of impaired astrocyte-neuron interaction, based on the role of the "glutamate/glutamine cycle" in the shuttling and recycling of Glu/GABA between astrocytes and neurons (Pereira et al., 2008; Xu et al., 2016), and may be further suggestive of the disruption of the astrocyte-neuron interaction by PFAS.

At the subcellular and molecular level, two interrelated targets of PFAS (including PFOA) have been most frequently identified: namely, (1) disruption of mitochondria, and (2) pathways associated with activation of peroxisome proliferator-activated receptors (PPAR). Multiple studies in cell-based systems have shown that PFOA causes mitochondrial dysfunction including swelling and disruption of membrane integrity, membrane potential collapse with disruption of the electron transport chain, and consequent reduction in ATP levels (Choi et al., 2017; Mashayekhi et al., 2015; Suh et al., 2017) At the same time, mitochondrial dysfunction has been linked to the induction of oxidative stress by PFOA (including studies in the zebrafish model; Hagenaars et al., 2013). Molecular studies, on the other hand, have consistently documented the activation of PPAR - and in particular, the PPARα and PPARγ subtypes - by PFOA (Abbott et al., 2012; Buhrke et al., 2013; Kennedy et al., 2004; Takacs and Abbott, 2006; Vanden Heuvel et al.,

2006). Collectively, the PPAR have diverse roles in lipid and glucose metabolism including β-oxidation, lipid biosynthesis and transport, ketogenesis, adipogenesis, and glucose homeostasis (i.e., glucose biosynthesis, catabolism, storage and transport) (Dubois et al., 2017; Peeters and Baes, 2010; Tan et al., 2005). Co-targeting of mitochondria and PPAR by PFOA is highly interrelated as both have key functions in cellular energetics as it relates, in particular, to carbohydrate (i.e., glucose) and lipid metabolism, and consequently, metabolic syndrome (Alderete et al., 2019; Cardenas et al., 2018; Christensen et al., 2019; Lin et al., 2009). Indeed, the alteration of numerous metabolites observed in the present study, likewise, points to the co-targeting of mitochondria and PPAR-regulated pathways as reflected by both apparent oxidative stress responses and impairment of cellular energetics including pathways relevant to metabolic syndrome, e.g., carbohydrate and glucose metabolism (Fig. 5). Alterations in metabolic profiles in relation to these two targets – as part of an integrated model - are discussed separately below.

3.3.1. Apparent disruption of mitochondrial pathways by PFAS

Several of the changes in metabolite profiles of PFAS-exposed zebrafish observed in the present study align with mitochondrial dysfunction in association with toxicity. Consistent with a compromise of mitochondrial membrane integrity, as previously established for PFOA (Hagenaars et al., 2013), significant increases in choline and glycerophosphocholine (GPC) were observed, and are possibly indicative of release and hydrolysis of phospholipids - following presumptive disruption of mitochondrial membranes – including, in particular, phosphatidylcholine as one of the most abundant (and typically most abundant) classes of lipids in mitochondrial membranes (Almaida-Pagán et al., 2014; de Kroon et al., 1997). Increased concentration of polar head-groups of membrane phospholipids (e.g., choline, GPC, ethanolamine, myo-inositol) as, likewise, measured by HRMAS NMR of intact zebrafish embryos has, in fact, been similarly linked in previous studies to membrane disruption in this system (Berry et al., 2016; Roy et al., 2017; Zuberi et al., 2019).

Most conspicuously, alteration of several metabolites associated with the tricarboxylic acid (TCA, or “citric acid”) cycle, and associated electron transport chain and oxidative phosphorylation, is directly aligned with disruption of mitochondria. Key changes associated with PFAS exposure, in this regard, include significant decreases in citrate and succinate, and increase of malate, as well as apparent metabolic accumulation of acetate, which generally indicate disruption of the TCA cycle, and an inability of carbon (via acetyl CoA) to enter the cycle (Fig. 5). Reductions in citrate and succinate, and increase in malate, which are associated with irreversible steps specifically point to inhibition of the aldol condensation of acetyl CoA and OAA as entry point (which, in turn, links glycolysis and β-oxidation) to the TCA cycle. Exclusively for PFO3TDA, fumarate was additionally increased, and likely reflects consequent upstream metabolic accumulation (from malate to fumarate) owing to the higher toxicity (and associated mitochondrial disruption) of this compound. Alongside changes in TCA cycle metabolites, significant decreases in the energetic currencies of NADH and ATP would correlate with inhibited yield of the former, and consequent lack of availability of this reducing agent for oxidative phosphorylation to produce the latter (Fig. 5).

Upstream of the TCA cycle, the observed alteration of metabolites associated with glycolysis and β-oxidation (which supply acetate to the TCA cycle) similarly indicate mitochondrial dysfunction and/or impairment of the transport of metabolic intermediates (from cytosol to the mitochondria) as part of these pathways (Fig. 5). Aerobic glycolysis in the cytosol, for example, provides pyruvate that is, in turn, transported to mitochondria where conversion by pyruvate dehydrogenase (PDH) within the mitochondrial matrix provides acetyl CoA for entry to the TCA cycle. The observed increase in pyruvate, therefore, may extend the metabolic accumulation (from acetate) associated with loss of TCA cycle function, and PDH activity. With respect to β-oxidation, one particularly telling response for the two most toxic PFAS (i.e., PFOA and PFO3TDA) may be a significant decrease in carnitine. Carnitine is essential to the transport of fatty acids (via coenzyme A-activated, i.e., acyl CoA, intermediates) whereby carnitine palmitoyltransferases (CPT) located in the outer and inner mitochondrial membranes (i. e., CPT I and II, respectively), catalyze formation of acyl carnitines for transport into the mitochondrial matrix (where β-oxidation of FA occurs), and subsequent recycling of carnitine (back to the cytosol). Decreased carnitine, therefore, likely reflects a decrease in the mitochondrial capacity for β-oxidation, and consequently diminished recycling of free carnitine, for these two most toxic PFAS (Fig. 5).

Alongside alterations of TCA cycle intermediates and precursors, auxiliary pathways are also seemingly affected by PFAS presumably due to impaired mitochondrial function. For example, in addition to their role in neurotransmitter recycling, Glu and Gln are important metabolic intermediates for entry to the TCA: cytosolic Gln is transported to the mitochondria, and converted within the mitochondrial matrix to Glu (by glutaminase) which can, in turn, enter the TCA cycle via α-ketoglutarate (αKG). Accordingly, the observed increase in Gln/Glu ratio is consistent with disruption of mitochondria. At the same time, Pro derived from collagen in the extracellular matrix during times of metabolic stress can be catabolized to Glu (to supply anaplerotic αKG to the TCA cycle) by proline oxidase (POX) which is localized to the inner membrane of the mitochondria (Phang et al., 2008). Thus, the significant increase in Pro, likewise, aligns with mitochondrial dysfunction, and specifically loss of POX activity (Fig. 5).

Finally, with respect to the role of mitochondria, previous studies have generally linked PFAS to increased production of reactive oxygen species (ROS) and consequent oxidative stress due to mitochondrial dysfunction (Liu et al., 2007; Suh et al., 2017; Wielsøe et al., 2015). Additionally, PFOA has been shown to decrease levels of nuclear factor erythroid 2-related factor (Nrf2) which is a key transcription factor required for induction of numerous genes involved in antioxidant response including GSH biosynthesis (Liu et al., 2015). The observed decrease in GSH for PFAS exposures would, therefore, generally align with both oxidative stress (i.e., production of ROS) and consequent depletion of the peptide, as well as reduced biosynthesis (via Nrf2). A similar decrease in GSH has, in fact, been consistently observed in association with PFOA-induced oxidative stress (Liu et al., 2007). In parallel, a marked increase in taurine was, furthermore, observed for all PFAS in the present study. Taurine has an established role in antioxidant defenses (Schaffer et al., 2009), and likewise, may indicate an upregulation in response to oxidative stress in zebrafish embryos. Moreover, taurine is associated with Nrf2 translocation (Sun et al., 2018), and therefore, may be directly involved in the upregulation of antioxidant responses.

3.3.2. Role of PPAR-regulated pathways in metabolic disruption by PFAS

Alongside mitochondria, PPAR has been consistently demonstrated to be a key target in PFAS toxicity. As transcription factors, PPAR are involved in the expression – specifically via PPAR response elements (PPRE) - of a wide range of genes, and accordingly, diverse cellular and biochemical pathways. However, the best described functions involve regulation of energy homeostasis including carbohydrate and lipid metabolism, and targeting of

PPAR would, in turn, support a reported contribution of PFAS in increased rates of obesity, diabetes and other related metabolic disorders (Liu et al., 2018). Although PPAR expression was not directly measured in the present study, numerous alterations of metabolic profiles by PFAS (described below) are consistent with a role of PPAR-regulated pathways.

Fatty acids are recognized as endogenous ligands for PPAR, and thereby, represent a direct link between PPAR and lipid metabolism, specifically via β-oxidation. As a proposed mechanism of action, PFOA have been shown to bind and activate PPAR (Vanden Heuvel et al., 2006; Yamamoto et al., 2014), and induce β-oxidation of fatty acids (Kudo et al., 2006; Yu et al., 2016). An expected decrease in fatty acids (via induction of β-oxidation), however, was only observed for PFO3TDA (Fig. 4) as the most toxic of the PFAS investigated. That said, any PPAR-directed induction of β-oxidation would likely be confounded by concomitant disruption of mitochondria (where β-oxidation occurs) by PFAS. Presumptive mitochondrial disruption may, thus, explain a lack of significant alteration in fatty acids (except for the most toxic PFO3TDA) due to impaired carnitine-based fatty acid transport pathways (as suggested by elevated carnitine levels observed here). Alongside a direct role in the catabolism (i.e., β-oxidation) of fatty acids, however, PPAR have also been shown to regulate lipid metabolism via other direct and indirect routes. Most notably, PPAR have been shown to regulate multiple pathways associated with metabolism and transport of cholesterol (Li and Chiang, 2009). Significant decrease in cholesterol with PFOA and PFO3TDA treatment observed in the present study (Fig. 4) may, therefore, be explained by the effect of these PFAS on PPAR-mediated pathways of cholesterol metabolism and uptake.

Although PPAR has been perhaps most widely investigated with respect to lipid metabolism, considerable evidence supports diverse roles in the regulation of glucose metabolism including glycolysis, gluconeogenesis and glycogen metabolism (Peeters and Baes, 2010). And concomitantly, multiple studies have suggested a role of altered glucose metabolism in the adverse effects of PFOA (Yan et al., 2015; Zheng et al., 2017). Activation of PPARγ by the agonist fenofibrate, for example, was previously shown (Oosterveer et al., 2009) to reduce glycolytic flux of glucose (via G6P) through glucokinase (i.e., hexokinase IV), as a key step in glycolysis, with diversion toward gluconeogenesis. At the same time, studies (Im et al., 2011) identified a PPRE within glucose-6-phosphatase (G6Pase), and demonstrated that PPARα upregulates this enzymes as the key final step in liver gluconeogenesis. Accordingly, PFAS activation of PPAR would be, likewise, expected to reduce G6P and increase glucose due to reduced glycolytic flux and/or upregulation of gluconeogenesis. Increased glucose was, indeed, observed for all PFAS evaluated in the present study (Fig. 4). A significant elevation in glucose was accompanied, in the case of PFO3TDA, by a decrease in lactate which may further reflect a decrease in glycolytic flux – and specifically anaerobic glycolysis (with lactate as end product) – or alternatively, increased hepatic gluconeogenesis from lactate (e.g., Cori cycle). That said, although a concomitant decrease in G6P (along with increased glucose) was observed for PFOA, this was not the case for either PFECA (Fig. 4).

In contrast to PFOA, PFO3TDA was actually found to increase G6P (rather than decrease as observed for PFOA), and taken together with a decrease in glucose-1-phosphate (G1P) that was, likewise, exclusively observed for PFO3TDA exposures, points to a possible role of glycogen metabolism in the case of this more toxic PFAS. Indeed, alongside glucose anabolism (i.e., gluconeogenesis) and catabolism (i.e., glycolysis), PFAS have been shown in multiple studies to alter glycogen metabolism. Specifically, PFOA was found to decrease liver glycogen with a concurrent increase in G6Pase as the final step in glycogenolysis, and decrease in glycogen synthase (GS) as the key regulatory step of glycogenesis (Zheng et al., 2017). Both of these enzymes, in turn, have been shown to be regulated by PPAR (Im et al., 2011; Mandard et al., 2007). More recently, PFOA was found to significantly decrease in glycogen (Hagenaars et al., 2013). Although a precise mechanistic role of PPAR in regulating glycogen metabolism remains unclear (Bandsma et al., 2004; Mandard et al., 2007; Oosterveer et al., 2009; Peeters and Baes, 2010), G1P is more or less exclusively associated with glycogenolysis (and, in reverse, glycogenesis), such that the concurrent increase in G1P, G6P and glucose for PFO3TDA-exposed embryos is highly consistent with a role of increased glycogenolysis (in relation to the higher toxicity of this variant). The increase of G6P (from glycogenolysis) could, in turn, offset any expected decreases of this metabolite resulting from reduced glycolytic flux and/or increased gluconeogenesis (as discussed above). Of additional note, the increase in G6P (exclusively for PFO3TDA-exposed embryos) is mirrored by a similarly unique increase in *myo*-inositol (Fig. 4) for which G6P is the rate-limiting biosynthetic substrate.

Although exposure to GenX did significantly increase glucose, none of the intermediates associated with glucose or glycogen metabolism, on the other hand, were significantly altered. It is proposed that elevated glucose, in this case, may be related instead to intercellular glucose transport, and the established role of PPAR in the expression of glucose transporters. Numerous studies, indeed, have shown that PPAR activation upregulates expression and/or translocation of bidirectional glucose transport (GLUT) proteins including, in particular, GLUT2 in the liver as the primary transporter of glucose between liver and blood (Dasgupta and Rai, 2018; Im et al., 2005; Kim and Ahn, 2004; Liao et al., 2007; Variya et al., 2019; Wu et al., 1998). Consistent with effects on glucose transport, PFOA exposure was previously found (in a mouse liver model) to decrease glucose in liver, while simultaneously increasing blood glucose, by directing hepatic glucose away from glycogen synthesis, and into the bloodstream toward other systems including various non-glycogen synthesizing cells, thus effectively increasing total "free" glucose (Zheng et al., 2017). Though only total glucose, and not cell-specific levels, in zebrafish embryos were measured in the present study, increased GLUT2 may, therefore, alternatively (in the case of GenX) or additionally explain observed elevation of glucose as a result of "escape" from hepatic glycogenesis (Fig. 6).

On this note, one of the most revealing differences in metabolic profiles between PFOA and PFECA is the relative changes in BCAA which are, in fact, well documented regulators of GLUT (Holeček, 2018; Zhang et al., 2017) and in turn, known to be regulated by PPAR. As essential amino acids, levels of BCAA are exclusively regulated by catabolism which takes place by a two-step process involving (1) the reversible conversion of BCAA to corresponding α-keto acids by BCAA amino transferases (BCAT) in extrahepatic cells, and (2) the subsequent rate-limiting irreversible decarboxylation by branched-chain keto acid dehydrogenase (BCKDH), primarily in hepatocytes, following transport of α-keto acids to the liver (Li et al., 2017). Both enzymes have been shown to be upregulated by activation of PPARγ, and downregulated when PPARγ genes are knocked-out (Blanchard et al., 2018). Enzymes involved in both steps, however, are either exclusively (i.e., BCKDH) or primarily localized to mitochondria (García-Espinosa et al., 2007; Holeček, 2018). In the case of PFOA, all BCAA were significantly increased, and it is proposed that mitochondrial disruption, therefore, may supersede PPAR-mediated effects (i.e., increased BCAA catabolism) whereby impairment of mitochondrial BCKDH would reduce catabolism, and consequently lead to the observed accumulation, of BCAA (which could, in turn, upregulate GLUT, and contribute to the observed increase in glucose).

In contrast to PFOA, however, BCAA were either not significantly

altered (i.e., leucine, isoleucine), or decreased to a lesser extent (i.e., valine), by both PFO3TDA and GenX (Fig. 4). In light of presumptive mitochondrial disruption (and consequent loss of BCAT and BCKDH catabolic activity which would be expected to increase BCAA levels), the lack of altered BCAA levels by PFECA may imply otherwise increased BCAA catabolism. In this regard, although BCAT is mostly localized to the mitochondria, cytosolic BCAT is abundant in certain cell types including, in particular, the CNS (García-Espinosa et al., 2007), where the first step of catabolism could, thus, consequently occur despite mitochondrial disruption (and loss of BCKDH activity). Further aligned with a possible increase in BCAA catabolism, alanine levels were also uniquely increased for both PFECA (but not PFOA); during transamination by BCAT, the amino group from glutamate (following deamination of BCAA) is transferred to alanine, and thus, increased BCAA catabolism would, indeed, be expected to increase alanine. At the same time, the observed increase in NAD^+ for PFECA-exposed embryos (and not PFOA) may reflect an upregulated BCAA catabolism by BCAT (in the absence of mitochondrial BCKDH). Specifically, it has been shown (Islam et al., 2010; Hutson et al., 2011) that in the absence of BCKDH activity, NAD^+ (which would, otherwise, be recycled to NADH in the presence of BCKDH) accumulates. Differences in the alteration of BCAA levels (and associated metabolites, i.e., alanine, NAD^+) between PFECA and PFOA may, therefore, point to differences in their effects on catabolic pathways including cell-specificity, or differential degrees of interaction (i.e., activation) with PPAR (increasing BCAA catabolism), compared to mitochondrial disruption (decreasing BCAA catabolism), or alternatively, toward particular subtypes, i.e., PPARα versus PPARγ. These hypotheses, however, remain to be investigated.

Finally, it is noteworthy that cysteine levels are uniquely decreased in embryos exposed to PFECA. Pathways targeted by PFECA with respect to the observed alteration of cysteine are not immediately clear. Cysteine has been linked to obesity, however, and depletion of cysteine was found to prevent induction of PPARγ and adipose differentiation (Haj-Yasein et al., 2017). At the same time, evidence suggests a role of PPARγ in the regulation of genes involved in biosynthesis including cystathionine γ-lyase (Yang et al., 2018) and cystathionine β-synthase (Mishra et al., 2010). It is possible that differential effects in relation to cysteine may, likewise, be linked to differences between PFOA and PFECA in terms of interactions with PPAR (and/or subtypes). However, these possibilities similarly remain to be investigated.

4. Conclusions

In conclusion, our findings confirm that PFECA are quantitatively and qualitatively (with respect to metabolic alterations) similar in toxicity to PFOA, as a “legacy” PFAS, in the zebrafish embryo system. Metabolic alterations are, furthermore, consistent with a previously reported link between PFAS and hepatotoxicity, neurotoxicity and metabolic syndrome including roles of mitochondria and PPAR, and may represent a model system for investigating this linkage. These findings most generally suggest that these next-generation PFAS need to be equally considered as environmental toxicants of potential concern.

Declaration of competing interest

The authors declare that they have no known competing financial interests or personal relationships that could have appeared to influence the work reported in this paper.

CRediT authorship contribution statement

Kiflom Y. Gebreab: Conceptualization, Methodology, Formal analysis, Investigation, Writing - original draft, Writing - review & editing, Visualization. **Muhamed N.H. Eeza:** Formal analysis, Investigation, Visualization. **Tianyu Bai:** Formal analysis, Investigation. **Zain Zuberi:** Formal analysis, Investigation. **Jörg Matysik:** Methodology, Resources. **Kevin E. O'Shea:** Conceptualization, Writing - original draft. **A. Alia:** Methodology, Formal analysis, Investigation, Resources, Writing - original draft, Writing - review & editing, Visualization, Supervision. **John P. Berry:** Conceptualization, Methodology, Formal analysis, Resources, Writing - original draft, Writing - review & editing, Visualization, Project administration, Funding acquisition.

Acknowledgments

The authors would like to thank Dr. Patrick Gibbs from the University of Miami Rosenstiel School of Marine and Atmospheric Science for providing zebrafish embryos used in primary toxicity assays. Likewise, the authors thank Dr. Stefan Scholz of the Helmholtz Center for Environmental Research-UFZ (Leipzig, Germany) who supplied zebrafish embryos in support of HRMAS NMR metabolic profiling studies. Finally, the authors would like to acknowledge support from Florida International University's Graduate School, and specifically the Presidential Fellowship program, which, in part, financially supported KG.

Appendix A. Supplementary data

Supplementary data to this article can be found online at https://doi.org/10.1016/j.envpol.2020.114928.

References

Abbott, B.D., Wood, C.R., Watkins, A.M., Tatum-Gibbs, K., Das, K.P., Lau, C., 2012. Effects of perfluorooctanoic acid (PFOA) on expression of peroxisome proliferator-activated receptors (PPAR) and nuclear receptor-regulated genes in fetal and postnatal CD-1 mouse tissues. Reprod. Toxicol. 33, 491–505.

Alderete, T.L., Jin, R., Walker, D.I., Valvi, D., Chen, Z., Jones, D.P., Peng, C., Gilliland, F.D., Berhane, K., Conti, D.V., 2019. Perfluoroalkyl substances, metabolomic profiling, and alterations in glucose homeostasis among overweight and obese Hispanic children: a proof-of-concept analysis. Environ. Int. 126, 445–453.

Alfieri, A., Malito, E., Orru, R., Fraaije, M.W., Mattevi, A., 2008. Revealing the moonlighting role of NADP in the structure of a flavin-containing monooxygenase. Proc. Natl. Acad. Sci. Unit. States Am. 105, 6572–6577.

Almaida-Pagán, P.F., Lucas-Sanchez, A., Tocher, D.R., 2014. Changes in mitochondrial membrane composition and oxidative status during rapid growth, maturation and aging in zebrafish, Danio rerio. Biochim. Biophys. Acta Mol. Cell Biol. Lipids 1841, 1003–1011.

Anderson, J.K., Luz, A.L., Goodrum, P., Durda, J., 2019. Perfluorohexanoic acid toxicity, part II: application of human health toxicity value for risk characterization. Regul. Toxicol. Pharmacol. 103, 10–20.

Bandsma, R.H.J., van Dijk, T.H., ter Harmsel, A., Kok, T., Reijngoud, D.-J., Staels, B., Kuipers, F., 2004. Hepatic de novo synthesis of glucose 6-phosphate is not affected in peroxisome proliferator-activated receptor α-deficient mice but is preferentially directed toward hepatic glycogen stores after a short term fast. J. Biol. Chem. 279, 8930–8937.

Barrea, L., Annunziata, G., Muscogiuri, G., Laudisio, D., Di Somma, C., Maisto, M., Tenore, G.C., Colao, A., Savastano, S., 2019. Trimethylamine N-oxide, Mediterranean diet, and nutrition in healthy, normal-weight adults: also a matter of sex? Nutrition 62, 7–17.

Berghmans, S., Butler, P., Goldsmith, P., Waldron, G., Gardner, I., Golder, Z., Richards, F.M., Kimber, G., Roach, A., Alderton, W., 2008. Zebrafish based assays for the assessment of cardiac, visual and gut function—potential safety screens for early drug discovery. J. Pharmacol. Toxicol. Methods 58, 59–68.

Berry, J.P., Gantar, M., Gibbs, P.D.L., Schmale, M.C., 2007. The zebrafish (Danio rerio) embryo as a model system for identification and characterization of developmental toxins from marine and freshwater microalgae. Comp. Biochem. Physiol. C Toxicol. Pharmacol. 145, 61–72.

Berry, J.P., Roy, U., Jaja-Chimedza, A., Sanchez, K., Matysik, J., Alia, A., 2016. High-resolution magic angle spinning nuclear magnetic resonance of intact zebrafish embryos detects metabolic changes following exposure to teratogenic

polymethoxyalkenes from algae. Zebrafish 13, 456–465.
Blanchard, P.-G., Moreira, R.J., Castro, É., Caron, A., Côté, M., Andrade, M.L., Oliveira, T.E., Ortiz-Silva, M., Peixoto, A.S., Dias, F.A., 2018. PPARγ is a major regulator of branched-chain amino acid blood levels and catabolism in white and brown adipose tissues. Metabolism 89, 27–38.
Buhrke, T., Kibellus, A., Lampen, A., 2013. In vitro toxicological characterization of perfluorinated carboxylic acids with different carbon chain lengths. Toxicol. Lett. 218, 97–104.
Cardenas, A., Hauser, R., Gold, D.R., Kleinman, K.P., Hivert, M.-F., Fleisch, A.F., Lin, P.-I.D., Calafat, A.M., Webster, T.F., Horton, E.S., 2018. Association of perfluoroalkyl and polyfluoroalkyl substances with adiposity. JAMA Netw. Open 1 e181493–e181493.
Chatzopoulou, A., Roy, U., Meijer, A.H., Alia, A., Spaink, H.P., Schaaf, M.J.M., 2015. Transcriptional and metabolic effects of glucocorticoid receptor α and β signaling in zebrafish. Endocrinology 156, 1757–1769.
Cheng, X., Klaassen, C.D., 2008. Critical role of PPAR-α in perfluorooctanoic acid–and perfluorodecanoic acid–induced downregulation of Oatp uptake transporters in mouse livers. Toxicol. Sci. 106, 37–45.
Choi, E.M., Suh, K.S., Rhee, S.Y., Oh, S., Woo, J.-T., Kim, S.W., Kim, Y.S., Pak, Y.K., Chon, S., 2017. Perfluorooctanoic acid induces mitochondrial dysfunction in MC3T3-E1 osteoblast cells. J. Environ. Sci. Health Part A 52, 281–289.
Christensen, K.Y., Raymond, M., Meiman, J., 2019. Perfluoroalkyl substances and metabolic syndrome. Int. J. Hyg. Environ. Health 222, 147–153.
Dasgupta, S., Rai, R.C., 2018. PPAR-γ and Akt regulate GLUT1 and GLUT3 surface localization during Mycobacterium tuberculosis infection. Mol. Cell. Biochem. 440, 127–138.
de Koning, C., Beekhuijzen, M., Tobor-Kapłon, M., de Vries-Buitenweg, S., Schoutsen, D., Leeijen, N., van de Waart, B., Emmen, H., 2015. Visualizing compound distribution during zebrafish embryo development: the effects of lipophilicity and DMSO. Birth Defects Res. Part B Dev. Reproductive Toxicol. 104, 253–272.
de Kroon, A.I.P.M., Dolis, D., Mayer, A., Lill, R., de Kruijff, B., 1997. Phospholipid composition of highly purified mitochondrial outer membranes of rat liver and Neurospora crassa. Is cardiolipin present in the mitochondrial outer membrane? Biochim. Biophys. Acta Biomembr. 1325, 108–116.
DeWitt, J.C., 2015. Toxicological Effects of Perfluoroalkyl and Polyfluoroalkyl Substances. Springer.
Ding, G., Zhang, J., Chen, Y., Wang, L., Wang, M., Xiong, D., Sun, Y., 2013. Combined effects of PFOS and PFOA on zebrafish (Danio rerio) embryos. Arch. Environ. Contam. Toxicol. 64, 668–675.
Domingo, J.L., Nadal, M., 2017. Per- and polyfluoroalkyl substances (PFASs) in food and human dietary intake: a review of the recent scientific literature. J. Agric. Food Chem. 65, 533–543.
Dubois, V., Eeckhoute, J., Lefebvre, P., Staels, B., 2017. Distinct but complementary contributions of PPAR isotypes to energy homeostasis. J. Clin. Invest. 127, 1202–1214.
Fair, P.A., Wolf, B., White, N.D., Arnott, S.A., Kannan, K., Karthikraj, R., Vena, J.E., 2019. Perfluoroalkyl substances (PFASs) in edible fish species from Charleston Harbor and tributaries, South Carolina, United States: exposure and risk assessment. Environ. Res. 171, 266–271.
García-Espinosa, M.A., Wallin, R., Hutson, S.M., Sweatt, A.J., 2007. Widespread neuronal expression of branched-chain aminotransferase in the CNS: implications for leucine/glutamate metabolism and for signaling by amino acids. J. Neurochem. 100, 1458–1468.
Giesy, J.P., Kannan, K., 2001. Global distribution of perfluorooctane sulfonate in wildlife. Environ. Sci. Technol. 35, 1339–1342.
Hagenaars, A., Vergauwen, L., Benoot, D., Laukens, K., Knapen, D., 2013. Mechanistic toxicity study of perfluorooctanoic acid in zebrafish suggests mitochondrial dysfunction to play a key role in PFOA toxicity. Chemosphere 91, 844–856.
Hagenaars, A., Vergauwen, L., De Coen, W., Knapen, D., 2011. Structure–activity relationship assessment of four perfluorinated chemicals using a prolonged zebrafish early life stage test. Chemosphere 82, 764–772.
Haj-Yasein, N.N., Berg, O., Jernerén, F., Refsum, H., Nebb, H.I., Dalen, K.T., 2017. Cysteine deprivation prevents induction of peroxisome proliferator-activated receptor gamma-2 and adipose differentiation of 3T3-L1 cells. Biochim. Biophys. Acta Mol. Cell Biol. Lipids 1862, 623–635.
H. Health, U.S.D. of, Services, 2018. Agency for Toxic Substances & Disease Registry (ATSDR). 2018.
Holeček, M., 2018. Branched-chain amino acids in health and disease: metabolism, alterations in blood plasma, and as supplements. Nutr. Metab. 15, 33.
Huang, H., Huang, C., Wang, L., Ye, X., Bai, C., Simonich, M.T., Tanguay, R.L., Dong, Q., 2010. Toxicity, uptake kinetics and behavior assessment in zebrafish embryos following exposure to perfluorooctanesulphonicacid (PFOS). Aquat. Toxicol. 98, 139–147.
Hutson, S.M., Islam, M.M., Zaganas, I., 2011. Interaction between glutamate dehydrogenase (GDH) and L-leucine catabolic enzymes: intersecting metabolic pathways. Neurochem. Int. 59, 518–524.
Im, S.-S., Kim, J.-W., Kim, T.-H., Song, X.-L., Kim, S.-Y., Kim, H., Ahn, Y.-H., 2005. Identification and characterization of peroxisome proliferator response element in the mouse GLUT2 promoter. Exp. Mol. Med. 37, 101.
Im, S.-S., Yousef, L., Blaschitz, C., Liu, J.Z., Edwards, R.A., Young, S.G., Raffatellu, M., Osborne, T.F., 2011. Linking lipid metabolism to the innate immune response in macrophages through sterol regulatory element binding protein-1a. Cell Metabol. 13, 540–549.
Islam, M.M., Nautiyal, M., Wynn, R.M., Mobley, J.A., Chuang, D.T., Hutson, S.M., 2010. Branched-chain amino acid metabolon interaction of glutamate dehydrogenase with the mitochondrial branched-chain aminotransferase (BCATm). J. Biol. Chem. 285, 265–276.
Jaja-Chimedza, A., Sanchez, K., Gantar, M., Gibbs, P., Schmale, M., Berry, J.P., 2017. Carotenoid glycosides from cyanobacteria are teratogenic in the zebrafish (Danio rerio) embryo model. Chemosphere 174, 478–489.
Janeiro, M.H., Ramírez, M.J., Milagro, F.I., Martínez, J.A., Solas, M., 2018. Implication of trimethylamine N-Oxide (TMAO) in disease: potential biomarker or new therapeutic target. Nutrients 10, 1398.
Jantzen, C.E., Annunziato, K.M., Cooper, K.R., 2016. Behavioral, morphometric, and gene expression effects in adult zebrafish (Danio rerio) embryonically exposed to PFOA, PFOS, and PFNA. Aquat. Toxicol. 180, 123–130.
Johansson, N., Fredriksson, A., Eriksson, P., 2008. Neonatal exposure to perfluorooctane sulfonate (PFOS) and perfluorooctanoic acid (PFOA) causes neurobehavioural defects in adult mice. Neurotoxicology 29, 160–169.
Kabli, S., Spaink, H.P., De Groot, H.J.M., Alia, A., 2009. In vivo metabolite profile of adult zebrafish brain obtained by high-resolution localized magnetic resonance spectroscopy. J. Magn. Reson. Imaging an off. J. Int. Soc. Magn. Reson. Med. 29, 275–281.
Keiter, S., Burkhardt-Medicke, K., Wellner, P., Kais, B., Färber, H., Skutlarek, D., Engwall, M., Braunbeck, T., Keiter, S.H., Luckenbach, T., 2016. Does perfluorooctane sulfonate (PFOS) act as chemosensitizer in zebrafish embryos? Sci. Total Environ. 548, 317–324.
KEMI, 2015. Occurrence and Use of Highly Fluorinated Substances and Alternatives.
Kennedy, G.L., Butenhoff, J.L., Olsen, G.W., O'Connor, J.C., Seacat, A.M., Perkins, R.G., Biegel, L.B., Murphy, S.R., Farrar, D.G., 2004. The toxicology of perfluorooctanoate. Crit. Rev. Toxicol. 34, 351–384.
Kim, H., Ahn, Y., 2004. Role of peroxisome proliferator-activated receptor-γ in the glucose-sensing apparatus of liver and β-cells. Diabetes 53, S60–S65.
Kimura, O., Fujii, Y., Haraguchi, K., Kato, Y., Ohta, C., Koga, N., Endo, T., 2017. Uptake of perfluorooctanoic acid by Caco-2 cells: involvement of organic anion transporting polypeptides. Toxicol. Lett. 277, 18–23.
Knöbel, M., Busser, F.J.M., Rico-Rico, A., Kramer, N.I., Hermens, J.L.M., Hafner, C., Tanneberger, K., Schirmer, K., Scholz, S., 2012. Predicting adult fish acute lethality with the zebrafish embryo: relevance of test duration, endpoints, compound properties, and exposure concentration analysis. Environ. Sci. Technol. 46, 9690–9700.
Kudo, N., Suzuki-Nakajima, E., Mitsumoto, A., Kawashima, Y., 2006. Responses of the liver to perfluorinated fatty acids with different carbon chain length in male and female mice: in relation to induction of hepatomegaly, peroxisomal β-oxidation and microsomal 1-acylglycerophosphocholine acyltransferase. Biol. Pharm. Bull. 29, 1952–1957.
Lang, D., Yeung, C., Peter, R., Ibarra, C., Gasser, R., Itagaki, K., Philpot, R., Rettie, A., 1998. Isoform specificity of trimethylamine N-oxygenation by human flavin-containing monooxygenase (FMO) and P450 enzymes: selective catalysis by FMO3. Biochem. Pharmacol. 56, 1005–1012.
Lau, C., Anitole, K., Hodes, C., Lai, D., Pfahles-Hutchens, A., Seed, J., 2007. Perfluoroalkyl acids: a review of monitoring and toxicological findings. Toxicol. Sci. 99, 366–394.
Li, T., Chiang, J.Y.L., 2009. Regulation of bile acid and cholesterol metabolism by PPARs. PPAR Res. 2009.
Li, T., Zhang, Z., Kolwicz Jr., S.C., Abell, L., Roe, N.D., Kim, M., Zhou, B., Cao, Y., Ritterhoff, J., Gu, H., 2017. Defective branched-chain amino acid catabolism disrupts glucose metabolism and sensitizes the heart to ischemia-reperfusion injury. Cell Metabol. 25, 374–385.
Liao, W., Nguyen, M.T.A., Yoshizaki, T., Favelyukis, S., Patsouris, D., Imamura, T., Verma, I.M., Olefsky, J.M., 2007. Suppression of PPAR-γ attenuates insulin-stimulated glucose uptake by affecting both GLUT1 and GLUT4 in 3T3-L1 adipocytes. Am. J. Physiol. Metab. 293, E219–E227.
Lin, C.-Y., Chen, P.-C., Lin, Y.-C., Lin, L.-Y., 2009. Association among serum perfluoroalkyl chemicals, glucose homeostasis, and metabolic syndrome in adolescents and adults. Diabetes Care 32, 702–707.
Liu, C., Yu, K., Shi, X., Wang, J., Lam, P.K.S., Wu, R.S.S., Zhou, B., 2007. Induction of oxidative stress and apoptosis by PFOS and PFOA in primary cultured hepatocytes of freshwater tilapia (Oreochromis niloticus). Aquat. Toxicol. 82, 135–143.
Liu, H.-S., Wen, L.-L., Chu, P.-L., Lin, C.-Y., 2018. Association among total serum isomers of perfluorinated chemicals, glucose homeostasis, lipid profiles, serum protein and metabolic syndrome in adults: NHANES, 2013–2014. Environ. Pollut. 232, 73–79.
Liu, W., Yang, B., Wu, L., Zou, W., Pan, X., Zou, T., Liu, F., Xia, L., Wang, X., Zhang, D., 2015. Involvement of NRF2 in perfluorooctanoic acid-induced testicular damage in male mice. Biol. Reprod. 93, 1–7, 41.
Liu, Yang, Wang, J., Liu, Yong, Zhang, H., Xu, M., Dai, J., 2009. Expression of a novel cytochrome P450 4T gene in rare minnow (Gobiocypris rarus) following perfluorooctanoic acid exposure. Comp. Biochem. Physiol. C Toxicol. Pharmacol. 150, 57–64.
Liu, Yong, Wang, J., Wei, Y., Zhang, H., Liu, Yang, Dai, J., 2008. Molecular characterization of cytochrome P450 1A and 3A and the effects of perfluorooctanoic acid on their mRNA levels in rare minnow (Gobiocypris rarus) gills. Aquat. Toxicol. 88, 183–190.
Maddox, J.F., Amuzie, C.J., Li, M., Newport, S.W., Sparkenbaugh, E., Cuff, C.F., Pestka, J.J., Cantor, G.H., Roth, R.A., Ganey, P.E., 2009. Bacterial-and viral-induced inflammation increases sensitivity to acetaminophen hepatotoxicity. J. Toxicol. Environ. Health Part A 73, 58–73.
Mahapatra, C.T., Damayanti, N.P., Guffey, S.C., Serafin, J.S., Irudayaraj, J.,

Sepúlveda, M.S., 2017. Comparative in vitro toxicity assessment of perfluorinated carboxylic acids. J. Appl. Toxicol. 37, 699–708.
Mamsen, L.S., Bjorvang, R.D., Mucs, D., Vinnars, M.T., Papadogiannakis, N., Lindh, C.H., Andersen, C.Y., Damdimopoulou, P., 2019. Concentrations of perfluoroalkyl substances (PFASs) in human embryonic and fetal organs from first, second, and third trimester pregnancies. Environ. Int. 124, 482–492.
Mandard, S., Stienstra, R., Escher, P., Tan, N.S., Kim, I., Gonzalez, F.J., Wahli, W., Desvergne, B., Müller, M., Kersten, S., 2007. Glycogen synthase 2 is a novel target gene of peroxisome proliferator-activated receptors. Cell. Mol. Life Sci. 64, 1145.
Mashayekhi, V., Tehrani, K.H.M.E., Hashemzaei, M., Tabrizian, K., Shahraki, J., Hosseini, M.J., 2015. Mechanistic approach for the toxic effects of perfluorooctanoic acid on isolated rat liver and brain mitochondria. Hum. Exp. Toxicol. 34, 985–996.
Matilla-Santander, N., Valvi, D., Lopez-Espinosa, M.-J., Manzano-Salgado, C.B., Ballester, F., Ibarluzea, J., Santa-Marina, L., Schettgen, T., Guxens, M., Sunyer, J., 2017. Exposure to perfluoroalkyl substances and metabolic outcomes in pregnant women: evidence from the Spanish INMA birth cohorts. Environ. Health Perspect. 125, 117004.
Mishra, P.K., Tyagi, N., Sen, U., Joshua, I.G., Tyagi, S.C., 2010. Synergism in hyperhomocysteinemia and diabetes: role of PPAR gamma and tempol. Cardiovasc. Diabetol. 9, 49.
Mortensen, A.S., Letcher, R.J., Cangialosi, M.V., Chu, S., Arukwe, A., 2011. Tissue bioaccumulation patterns, xenobiotic biotransformation and steroid hormone levels in Atlantic salmon (Salmo salar) fed a diet containing perfluoroactane sulfonic or perfluorooctane carboxylic acids. Chemosphere 83, 1035–1044.
Muratsubaki, H., Yamaki, A., 2011. Profile of plasma amino acid levels in rats exposed to acute hypoxic hypoxia. Indian J. Clin. Biochem. 26, 416–419.
Oosterveer, M.H., Grefhorst, A., van Dijk, T.H., Havinga, R., Staels, B., Kuipers, F., Groen, A.K., Reijngoud, D.-J., 2009. Fenofibrate simultaneously induces hepatic fatty acid oxidation, synthesis, and elongation in mice. J. Biol. Chem. 284, 34036–34044.
Pandya, M., Patel, D., Rana, J., Patel, M., Khan, N., 2016. Hepatotoxicity by acetaminophen and amiodarone in zebrafish embryos. J. Young Pharm. 8, 50.
Peeters, A., Baes, M., 2010. Role of PPAR. PPAR Res. 2010.
Peng, S., Yan, L., Zhang, J., Wang, Z., Tian, M., Shen, H., 2013. An integrated metabonomics and transcriptomics approach to understanding metabolic pathway disturbance induced by perfluorooctanoic acid. J. Pharmaceut. Biomed. Anal. 86, 56–64.
Pereira, F.C., Rolo, M.R., Marques, E., Mendes, V.M., Ribeiro, C.F., Ali, S.F., Morgadinho, T., Macedo, T.R., 2008. Acute increase of the glutamate–glutamine cycling in discrete brain areas after administration of a single dose of amphetamine. Ann. N. Y. Acad. Sci. 1139, 212–221.
Pérez, F., Nadal, M., Navarro-Ortega, A., Fàbrega, F., Domingo, J.L., Barceló, D., Farré, M., 2013. Accumulation of perfluoroalkyl substances in human tissues. Environ. Int. 59, 354–362.
Phang, J.M., Donald, S.P., Pandhare, J., Liu, Y., 2008. The metabolism of proline, a stress substrate, modulates carcinogenic pathways. Amino Acids 35, 681–690.
Popovic, M., Zaja, R., Fent, K., Smital, T., 2014. Interaction of environmental contaminants with zebrafish organic anion transporting polypeptide, Oatp1d1 (Slco1d1). Toxicol. Appl. Pharmacol. 280, 149–158.
Prevedouros, K., Cousins, I.T., Buck, R.C., Korzeniowski, S.H., 2006. Sources, fate and transport of perfluorocarboxylates. Environ. Sci. Technol. 40, 32–44.
Rotondo, J.C., Giari, L., Guerranti, C., Tognon, M., Castaldelli, G., Fano, E.A., Martini, F., 2018. Environmental doses of perfluorooctanoic acid change the expression of genes in target tissues of common carp. Environ. Toxicol. Chem. 37, 942–948.
Roy, U., Conklin, L., Schiller, J., Matysik, J., Berry, J.P., Alia, A., 2017. Metabolic profiling of zebrafish (Danio rerio) embryos by NMR spectroscopy reveals multifaceted toxicity of β-methylamino-L-alanine (BMAA). Sci. Rep. 7, 17305.
Schaffer, S.W., Azuma, J., Mozaffari, M., 2009. Role of antioxidant activity of taurine in diabetes. Can. J. Physiol. Pharmacol. 87, 91–99.
Shafique, U., Schulze, S., Slawik, C., Kunz, S., Paschke, A., Schüürmann, G., 2017. Gas chromatographic determination of perfluorocarboxylic acids in aqueous samples–A tutorial review. Anal. Chim. Acta 949, 8–22.
Shao, X., Ji, F., Wang, Y., Zhu, L., Zhang, Z., Du, X., Chung, A.C.K., Hong, Y., Zhao, Q., Cai, Z., 2018. Integrative chemical proteomics-metabolomics approach reveals Acaca/Acacb as direct molecular targets of PFOA. Anal. Chem. 90, 11092–11098.
Shrestha, S., Bloom, M.S., Yucel, R., Seegal, R.F., Rej, R., McCaffrey, R.J., Wu, Q., Kannan, K., Fitzgerald, E.F., 2017. Perfluoroalkyl substances, thyroid hormones, and neuropsychological status in older adults. Int. J. Hyg. Environ. Health 220, 679–685.
Song, Z., Zhou, Z., Chen, T., Hill, D., Kang, J., Barve, S., McClain, C., 2003. S-adenosylmethionine (SAMe) protects against acute alcohol induced hepatotoxicity in mice☆. J. Nutr. Biochem. 14, 591–597.
Steenland, K., Tinker, S., Frisbee, S., Ducatman, A., Vaccarino, V., 2009. Association of perfluorooctanoic acid and perfluorooctane sulfonate with serum lipids among adults living near a chemical plant. Am. J. Epidemiol. 170, 1268–1278.
Substances, A. for T., Registry, D., 2015. Draft Toxicological Profile for Perfluoroalkyls.
Suh, K.S., Choi, E.M., Kim, Y.J., Hong, S.M., Park, S.Y., Rhee, S.Y., Oh, S., Kim, S.W., Pak, Y.K., Choe, W., 2017. Perfluorooctanoic acid induces oxidative damage and mitochondrial dysfunction in pancreatic β-cells. Mol. Med. Rep. 15, 3871–3878.
Sun, M., Arevalo, E., Strynar, M., Lindstrom, A., Richardson, M., Kearns, B., Pickett, A., Smith, C., Knappe, D.R.U., 2016. Legacy and emerging perfluoroalkyl substances are important drinking water contaminants in the Cape fear river watershed of North Carolina. Environ. Sci. Technol. Lett. 3, 415–419. https://doi.org/10.1021/acs.estlett.6b00398.
Sun, Q., Jia, N., Yang, J., Chen, G., 2018. Nrf2 signaling pathway mediates the antioxidative effects of taurine against corticosterone-induced cell death in HUMAN SK-N-SH cells. Neurochem. Res. 43, 276–286.
Sunderland, E.M., Hu, X.C., Dassuncao, C., Tokranov, A.K., Wagner, C.C., Allen, J.G., 2019. A review of the pathways of human exposure to poly- and perfluoroalkyl substances (PFASs) and present understanding of health effects. J. Expo. Sci. Environ. Epidemiol. 29, 131–147.
Takacs, M.L., Abbott, B.D., 2006. Activation of mouse and human peroxisome proliferator–activated receptors (α, β/δ, γ) by perfluorooctanoic acid and perfluorooctane sulfonate. Toxicol. Sci. 95, 108–117.
Tan, G.D., Fielding, B.A., Currie, J.M., Humphreys, S.M., Desage, M., Frayn, K.N., Laville, M., Vidal, H., Karpe, F., 2005. The effects of rosiglitazone on fatty acid and triglyceride metabolism in type 2 diabetes. Diabetologia 48, 83–95.
Tang, J., Jia, X., Gao, N., Wu, Y., Liu, Z., Lu, X., Du, Q., He, J., Li, N., Chen, B., 2018. Role of the Nrf2-ARE pathway in perfluorooctanoic acid (PFOA)-induced hepatotoxicity in Rana nigromaculata. Environ. Pollut. 238, 1035–1043.
Ulhaq, M., Carlsson, G., Örn, S., Norrgren, L., 2013. Comparison of developmental toxicity of seven perfluoroalkyl acids to zebrafish embryos. Environ. Toxicol. Pharmacol. 36, 423–426.
van Amerongen, Y.F., Roy, U., Spaink, H.P., de Groot, H.J.M., Huster, D., Schiller, J., Alia, A., 2014. Zebrafish brain lipid characterization and quantification by 1H nuclear magnetic resonance spectroscopy and MALDI-TOF mass spectrometry. Zebrafish 11, 240–247.
Vanden Heuvel, J.P., Thompson, J.T., Frame, S.R., Gillies, P.J., 2006. Differential activation of nuclear receptors by perfluorinated fatty acid analogs and natural fatty acids: a comparison of human, mouse, and rat peroxisome proliferator-activated receptor-α,-β, and-γ, liver X receptor-β, and retinoid X receptor-α. Toxicol. Sci. 92, 476–489.
Variya, B.C., Bakrania, A.K., Patel, S.S., 2019. Antidiabetic potential of gallic acid from Emblica officinalis: improved glucose transporters and insulin sensitivity through PPAR-γ and Akt signaling. Phytomedicine 152906.
Vogs, C., Johanson, G., Näslund, M., Wulff, S., Sjödin, M., Hellstrandh, M., Lindberg, J., Wincent, E., 2019. Toxicokinetics of perfluorinated alkyl acids influences their toxic potency in the zebrafish embryo (Danio rerio). Environ. Sci. Technol. 53, 3898–3907.
Wang, Z., Cousins, I.T., Scheringer, M., Hungerbuehler, K., 2015. Hazard assessment of fluorinated alternatives to long-chain perfluoroalkyl acids (PFAAs) and their precursors: status quo, ongoing challenges and possible solutions. Environ. Int. 75, 172–179.
Wang, Z., Cousins, I.T., Scheringer, M., Hungerbühler, K., 2013. Fluorinated alternatives to long-chain perfluoroalkyl carboxylic acids (PFCAs), perfluoroalkane sulfonic acids (PFSAs) and their potential precursors. Environ. Int. 60, 242–248.
Wang, Z., DeWitt, J.C., Higgins, C.P., Cousins, I.T., 2017. A never-ending story of per- and polyfluoroalkyl substances (PFASs)?.
Weiss-Errico, M., Berry, J., O'Shea, K., 2017. β-Cyclodextrin attenuates perfluorooctanoic acid toxicity in the zebrafish embryo model. Toxics 5, 31.
Wen, W., Xia, X., Hu, D., Zhou, D., Wang, H., Zhai, Y., Lin, H., 2017. Long-chain perfluoroalkyl acids (PFAAs) affect the bioconcentration and tissue distribution of short-chain PFAAs in zebrafish (Danio rerio). Environ. Sci. Technol. 51, 12358–12368.
Wen, W., Xia, X., Zhou, D., Wang, H., Zhai, Y., Lin, H., Chen, J., Hu, D., 2019. Bioconcentration and tissue distribution of shorter and longer chain perfluoroalkyl acids (PFAAs) in zebrafish (Danio rerio): effects of perfluorinated carbon chain length and zebrafish protein content. Environ. Pollut. 249, 277–285.
Wielsøe, M., Long, M., Ghisari, M., Bonefeld-Jørgensen, E.C., 2015. Perfluoroalkylated substances (PFAS) affect oxidative stress biomarkers in vitro. Chemosphere 129, 239–245.
Worley, R.R., Moore, S.M., Tierney, B.C., Ye, X., Calafat, A.M., Campbell, S., Woudneh, M.B., Fisher, J., 2017. Per- and polyfluoroalkyl substances in human serum and urine samples from a residentially exposed community. Environ. Int. 106, 135–143.
Wu, Z., Xie, Y., Morrison, R.F., Bucher, N.L., Farmer, S.R., 1998. PPARgamma induces the insulin-dependent glucose transporter GLUT4 in the absence of C/EBPalpha during the conversion of 3T3 fibroblasts into adipocytes. J. Clin. Invest. 101, 22–32.
Xu, H., Zhang, H., Zhang, J., Huang, Q., Shen, Z., Wu, R., 2016. Evaluation of neuron-glia integrity by in vivo proton magnetic resonance spectroscopy: implications for psychiatric disorders. Neurosci. Biobehav. Rev. 71, 563–577.
Yamamoto, A., Kakuta, H., Sugimoto, Y., 2014. Involvement of glucocorticoid receptor activation on anti-inflammatory effect induced by peroxisome proliferator-activated receptor γ agonist in mice. Int. Immunopharm. 22, 204–208.
Yan, S., Zhang, H., Zheng, F., Sheng, N., Guo, X., Dai, J., 2015. Perfluorooctanoic acid exposure for 28 days affects glucose homeostasis and induces insulin hypersensitivity in mice. Sci. Rep. 5, 11029.
Yang, C.-H., Glover, K.P., Han, X., 2010. Characterization of cellular uptake of perfluorooctanoate via organic anion-transporting polypeptide 1A2, organic anion transporter 4, and urate transporter 1 for their potential roles in mediating human renal reabsorption of perfluorocarboxylates. Toxicol. Sci. 117, 294–302.
Yang, G., Ju, Y., Fu, M., Zhang, Y., Pei, Y., Racine, M., Baath, S., Merritt, T.J.S., Wang, R., Wu, L., 2018. Cystathionine gamma-lyase/hydrogen sulfide system is essential for adipogenesis and fat mass accumulation in mice. Biochim. Biophys. Acta Mol. Cell Biol. Lipids 1863, 165–176.
Yu, N., Wei, S., Li, M., Yang, J., Li, K., Jin, L., Xie, Y., Giesy, J.P., Zhang, X., Yu, H., 2016.

Effects of perfluorooctanoic acid on metabolic profiles in brain and liver of mouse revealed by a high-throughput targeted metabolomics approach. Sci. Rep. 6, 23963.
Zhang, S., Zeng, X., Ren, M., Mao, X., Qiao, S., 2017. Novel metabolic and physiological functions of branched chain amino acids: a review. J. Anim. Sci. Biotechnol. 8, 10.
Zhao, W., Zitzow, J.D., Weaver, Y., Ehresman, D.J., Chang, S.-C., Butenhoff, J.L., Hagenbuch, B., 2016. Organic anion transporting polypeptides contribute to the disposition of perfluoroalkyl acids in humans and rats. Toxicol. Sci. 156, 84–95.
Zheng, F., Sheng, N., Zhang, H., Yan, S., Zhang, J., Wang, J., 2017. Perfluorooctanoic acid exposure disturbs glucose metabolism in mouse liver. Toxicol. Appl. Pharmacol. 335, 41–48.
Zheng, X.-M., Liu, H.-L., Shi, W., Wei, S., Giesy, J.P., Yu, H.-X., 2012. Effects of perfluorinated compounds on development of zebrafish embryos. Environ. Sci. Pollut. Res. 19, 2498–2505.
Zuberi, Z., Eeza, M.N.H., Matysik, J., Berry, J.P., Alia, A., 2019. NMR-based metabolic profiles of intact zebrafish embryos exposed to aflatoxin B1 recapitulates hepatotoxicity and supports possible neurotoxicity. Toxins (Basel). 11, 258.